arXiv:2007.04160v1 [math.AG] 8 Jul 2020

An introduction to Lipschitz geometry of complex singularities

Anne Pichon

Abstract The aim of this paper to introduce the reader to a recent point of view on the Lipschitz classifications of complex singularities. It presents the complete classification of Lipschitz geometry of complex plane curves singularities and in particular, it introduces the so-called bubble trick, which is a key tool to study Lipschitz geometry of germs. It describes also the thick-thin decomposition of a normal complex surface singularity and built two geometric decompositions of a normal surface germ into standard pieces which are invariant by respectively inner and outer bilipschitz homeomorphisms. This leads in particular to the complete classification of Lipschitz geometry for the inner metric.

Introduction

The aim of this paper is to introduce the reader to a recent point of view on the Lipschitz classifications of complex singularities. It is an expansion of my notes prepared for the course given at the International school on singularities and Lipschitz geometry, which took place in Cuernavaca (Mexico) from June 11th to 22nd 2018.

The notes are structured as follows. Section 1 explains what is Lipschitz geometry for the inner and outer metrics of singularities and why it is interesting for the classification of space singularities. Section 2 gives the complete classification of Lipschitz geometry of complex curves and covers the results of [NP14]. In particular, it introduces what we call the bubble trick and the bubble trick with jumps, which are key tools to study Lipschitz geometry of germs. This techniques, which consists in exploring a germ of analytic space $(X,0)$ by using horns centered on a germ of real arc, was pioneered in [HP03] and used in several recent works (see e.g. [NP12, NP14, FdBHPPS19]). Section 3 describes the thick-thin decomposition of a

Anne Pichon
Aix Marseille Université, CNRS, Centrale Marseille, I2M, UMR 7373, 13453 Marseille, FRANCE
e-mail: anne.pichon@univ-amu.fr

normal complex surface germ following [BNP14]. Section 4 describes two geometric decompositions of a normal surface germ into standard pieces which are invariant by respectively inner and outer bilipschitz homeomorphism, following the results of [BNP14] and [NP12]. This leads in particular to the complete classification of Lipschitz geometry for the inner metric.

The paper contains a lot of detailed examples which were presented and discussed during the afternoon exercise sessions of the school and also an appendix (Part 5) which gives the computation of the resolution graph of a surface singularity with equation $x^2 + f(y,z) = 0$ following Hirzebruch-Jung and Laufer's method. This enables the readers to produce a lot of examples by themself.

In these notes, I do not give the detailed proofs of the invariance of the inner and outer Lipschitz decompositions (Theorem 4.30 and Theorem 4.36). We refer to [BNP14] and [NP12] respectively. However, it has to be noted that even if the two statements look similar, the techniques used in the proofs are radically different. The invariance of the inner decomposition uses the Lipschitz invariance of fast loops (introduced in Section 3) of minimal length in their homology class ([BNP14, Section 14]) while that of the outer invariance uses sophisticated bubble trick arguments ([NP12]).

Notice that the pioneering paper [BNP14] is written for a normal complex surface, as well as the initial version of [NP12]. However, the extensions of the inner and outer geometric decompositions to the general case of a reduced singularity (not necessarily isolated) are fairly easy. A version of [NP12] in this general setting will appear soon.

Finally, notice that the inner and outer geometric decompositions are the analogs of the pizza decompositions of a real surface germ. In the real surface case, these decompositions give complete classifications for the inner and outer metrics. As already mentioned, the inner decomposition in the complex case also gives a complete classification after adding a few more invariants (Theorem 4.30). In contrast, a complete classification for the outer metric of complex surface singularities would need more work and is still an open question.

1 Preliminaries

1.1 What is Lipschitz geometry of singular spaces?

In the sequel, $\mathbb{K}$ will denote either $\mathbb{R}$ or $\mathbb{C}$.

Let $(X,0)$ be a germ of analytic space in $\mathbb{K}^n$ which contains the origin. So X is defined by

$$X = \{(x_1,\dots,x_n) \in \mathbb{K}^n \mid f_j(x_1,\dots,x_n) = 0, j = 1,\dots,r\},$$

where the f_j's are convergent power series, $f_j \in \mathbb{K}\{x_1,\dots,x_n\}$ and $f_j(0) = 0$.

Question 1. How does X look in a small neighbourhood of the origin?

There are multiple answers to this vague question depending on the category we work in, i.e., on the chosen equivalence relation between germs.

First, we can consider the topological equivalence relation:

Definition 1.1. Two analytic germs $(X,0)$ and $(X',0)$ are **topologically equivalent** if there exists a germ of homeomorphism $\psi : (X,0) \to (X',0)$. The **topological type** of $(X,0)$ is the equivalence class of $(X,0)$ for this equivalence relation.

Two analytic germs $(X,0) \subset (\mathbb{K}^n,0)$ and $(X',0) \subset (\mathbb{K}^n,0)$ are **topologically equisingular** if there exists a germ of homeomorphism $\psi : (\mathbb{K}^n,0) \to (\mathbb{K}^n,0)$ such that $\psi(X) = X'$. We call **embedded topological type** of $(X,0)$ the equivalence class of $(X,0)$ for this equivalence relation.

The embedded topological type of $(X,0) \subset (\mathbb{R}^n,0)$ is completely determined by the embedded topology of its link as stated in the following famous Conical Structure Theorem:

Theorem 1.2 (Conical Structure Theorem). *Let B^n_ϵ be the ball with radius $\epsilon > 0$ centered at the origin of $\mathbb{R}^n$ and let S^{n-1}_ϵ be its boundary.*

Let $(X,0) \subset (\mathbb{R}^n,0)$ be an analytic germ. For $\epsilon > 0$, set $X^{(\epsilon)} = S^{n-1}_\epsilon \cap X$. There exists $\epsilon_0 > 0$ such that for every $\epsilon > 0$ with $0 < \epsilon \leq \epsilon_0$, the pair $(B^n_\epsilon, X \cap B^n_\epsilon)$ is homeomorphic to the pair $(B^n_{\epsilon_0}, Cone(X^{(\epsilon_0)}))$, where $Cone(X^{(\epsilon_0)})$ denotes the cone over $X^{(\epsilon_0)}$, i.e., the union of the segments $[0,x]$ joining the origin to a point $x \in X^{(\epsilon_0)}$.

In other words, the homeomorphism class of the pair $(S^{n-1}_\epsilon, X^{(\epsilon)})$ does not depend on ϵ when $\epsilon > 0$ is sufficiently small and it determines completely the embedded topological type of $(X,0)$.

Definition 1.3. When $0 < \epsilon \leq \epsilon_0$, the intersection $X^{(\epsilon)}$ is called the **link** of $(X,0)$.

Example 1.4. 1. Assume that X is the real cusp in $\mathbb{R}^2$ with equation $x^3 - y^2 = 0$. Then its link at 0 consists of two points in the circle S^1_ϵ.
2. If X is the complex cusp in $\mathbb{C}^2$ with equation $x^3 - y^2 = 0$, its link at 0 is the trefoil knot in the 3-sphere S^3_ϵ.
3. If X is the complex surface E_8 in $\mathbb{C}^3$ with equation $x^2 + y^3 + z^5 = 0$, its (non embedded) link at 0 is a Seifert manifold whose homeomorphism class is completely described through plumbing theory by its minimal resolution graph. The resolution graph is explicitely computed in the appendix 5 of the present notes.

The Conical Structure Theorem gives a complete answer to Question 1 in the topological category, but it completely ignores the geometric properties of the set $(X,0)$. In particular, a very interesting question is:

Question 2. How does the link $X^{(\epsilon)}$ evolve metrically as ϵ tends to 0?

In other words, is $X \cap B_\epsilon$ bilipschitz homeomorphic to the straight cone $Cone(X^{(\epsilon)})$? Or are there some parts of $X^{(\epsilon)}$ which shrink faster than linearly when ϵ tends to 0?

This question can be studied from different points of view depending on the choice of the metric. If $(X,0) \subset (\mathbb{R}^n,0)$ is the germ of a real analytic space, there are two natural metrics on $(X,0)$ which are defined from the Euclidean metric of the ambient space $\mathbb{R}^n$:

Definition 1.5. The **outer metric** d_o on X is the metric induced by the ambient Euclidean metric, i.e., for all $x, y \in X$, $d_o(x,y) = \|x-y\|_{\mathbb{R}^n}$.

The **inner metric** d_i on X is the length metric defined for all $x, y \in X$ by: $d_i(x,y) = \inf length(\gamma)$, where $\gamma\colon [0,1] \to X$ varies among rectifyable arcs on X such that $\gamma(0) = x$ and $\gamma(1) = y$.

Definition 1.6. Let (M,d) and (M',d') be two metric spaces. A map $f\colon M \to M'$ is a **bilipschitz homeomorphism** if f is a bijection and there exists a real constant $K \geq 1$ such that for all $x, y \in M$,

$$\frac{1}{K} d(x,y) \leq d'(f(x), f(y)) \leq K d(x,y).$$

Definition 1.7. Two real analytic germs $(X,0) \subset (\mathbb{R}^n,0)$ and $(X',0) \subset (\mathbb{R}^m,0)$ are **inner Lipschitz equivalent** (resp. **outer Lipschitz equivalent**) if there exists a germ of bilipschitz homeomorphism $\psi\colon (X,0) \to (X',0)$ with respect to the inner (resp. outer) metrics.

The equivalence classes of the germ $(X,0) \subset (\mathbb{R}^n,0)$ for these equivalence relations are called respectively the **inner Lipschitz geometry** and the **outer Lipschitz geometry** of $(X,0)$.

Throughout these notes, we will use the "big-Theta" asymptotic notations of Bachmann-Landau in the following form:

Definition 1.8. Given two function germs $f, g\colon ([0,\infty),0) \to ([0,\infty),0)$, we say that f is **big-Theta** of g and we write $f(t) = \Theta(g(t))$ if there exist real numbers $\eta > 0$ and $K > 0$ such that for all t such that for all $t \in [0,\eta)$, $\frac{1}{K} g(t) \leq f(t) \leq K g(t)$.

Example 1.9. Consider the real cusp C with equation $y^2 - x^3 = 0$ in $\mathbb{R}^2$ (see Figure 1). For a real number $t > 0$, consider the two points $p_1(t) = (t^2, t^3)$ and $p_2(t) = (t^2, -t^3)$ on C. Then $d_o(p_1(t), p_2(t)) = \Theta(t^{3/2})$ while the inner distance is obtained by taking infimum of lengths of paths on C between the two points $p_1(t)$ and $p_2(t)$. The shortest length is obtained by taking a path going through the origin, and we have $d_i(p_1(t), p_2(t)) = \Theta(t)$. Therefore, taking the limit of the quotient as t tends to 0, we obtain:

$$\frac{d_o(p_1(t), p_2(t))}{d_i(p_1(t), p_2(t))} = \Theta(t^{1/2}) \to 0.$$

Using this, you are ready to make the following:

Exercise 1.10. 1. Prove that there is no bilipschitz homeomorphism between the outer and inner metrics on the real cusp C with equation $y^2 - x^3 = 0$ in $\mathbb{R}^2$.

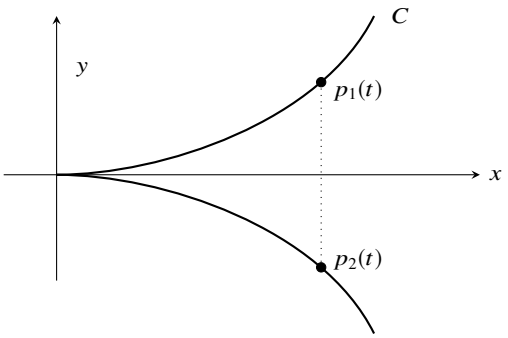


Fig. 1: The real cusp $y^2 - x^3 = 0$

2. Prove that $(C, 0)$ equipped with the inner metric is metrically conical, i.e. bilipschitz equivalent to the cone over its link.

Example 1.11. Consider the real surface S in $\mathbb{R}^3$ with equation $x^2 + y^2 - z^3 = 0$ in $\mathbb{R}^2$. For a real number $t > 0$, consider the two points $p_1(t) = (t^3, 0, t^2)$ and $p_2(t) = (t^3, 0, -t^2)$ on S. Then $d_o(p_1(t), p_2(t)) = \Theta(t^{3/2})$. We also have $d_i(p_1(t), p_2(t)) = \Theta(t^{3/2})$ since $d_i(p_1(t), p_2(t))$ is the length of a half-circle joining $p_1(t)$ and $p_2(t)$ on the circle $\{x = t^3\} \cap S$.

Exercise 1.12. Consider the real surface S of Example 1.11.

1. Prove that the identity map is a bilipschitz homeomorphism between the outer and inner metrics on $(S, 0)$.
2. Prove that $(S, 0)$ equipped with the inner metric is not metrically conical.

1.2 Independence of the embedding and motivations

If $(X, 0)$ is a germ of a real analytic space, the two metrics d_o and d_i defined above obviously depend on the choice of an embedding $(X, 0) \subset (\mathbb{R}^n, 0)$ since they are defined by using the Euclidean metric of the ambient $\mathbb{R}^n$. The aim of this section is to give a proof of one of the main results which motivates the study of Lipschitz geometry of singularities:

Proposition 1.13. *The Lipschitz geometries of* $(X, 0)$ *for the outer and inner metrics are independent of the embedding* $(X, 0) \subset (\mathbb{R}^n, 0)$.

In other words, bilipschitz classes of $(X, 0)$ just depend on the analytic type of $(X, 0)$. Before proving this result, let us give some consequences which motivate the study of Lipschitz geometry of germs of singular spaces.

The outer Lipschitz geometry determines the inner Lipschitz geometry since the inner metric is determined by the outer one through integration along paths.

Moreover, the inner Lipschitz geometry obviously determines the topological type of $(X, 0)$. Therefore, an important consequence of Proposition 1.13 is that the Lipschitz geometries give two intermediate classifications between the analytical type and the topological type.

A very small amount of analytic invariants are determined by the topological type of an analytic germ (even if one considers the embedded topological type). In particular, a natural question is to ask whether the Lipschitz classification is sufficiently rigid to catch analytic invariants:

Question 3. Which analytical invariants are in fact Lipschitz invariants?

Recent results show that in the case of a complex surface singularity, a large amount of analytic invariants are determined by the outer Lipschitz geometry. For example, the multiplicity of a complex surface singularity is an outer Lipschitz invariant ([NP12] for a normal surface, [Sam17] for a hypersurface in $\mathbb{C}^3$ and [FdBFS18] for the general case). However it is now known that the multiplicity is not a Lipschitz invariant in higher dimensions ([BFSV18]). In [NP12] it is shown that many other data are in fact Lipschitz invariants in the case of surface singularities, such as the geometry of hyperplane sections and the geometry of polar curves and discriminant curves of generic projections (Theorem 4.38); higher dimensions remain almost unexplored. This shows that the outer Lipschitz class contains potentially a lot of information on the singularity and that outer Lipschitz geometry of singularities is a very promising area to explore.

Here is another motivation. Analytic types of singular space germs contain continuous moduli, and this is why it is difficult to describe a complete analytic classification. For example, consider the family of curves germs $(X_t, 0)_{t\in\mathbb{C}}$ where X_t is the union of four transversal lines with equation $xy(x - y)(x - ty) = 0$. For every pair (t, t') with $t \neq t'$, $(X_t, 0)$ is not analytically equivalent to $(X_{t'}, 0)$. On the contrary, it is known since the works of T. Mostowki in the complex case ([Mos85]), and Parusiński in the real case ([Par88] and [Par94]), that the outer Lipschitz classification of germs of singular spaces is **tame**, which means that it admits a discrete complete invariant. Then a complete classification of Lipschitz geometry of singular spaces seems to be a more reachable goal.

Proof (of Proposition 1.13). Let $(f_1, \dots, f_n)$ and $(g_1, \dots, g_m)$ be two systems of generators of the maximal ideal $\mathcal{M}$ of $(X, 0)$. We will first prove that the outer metrics d_I and d_J for the embeddings

$$I = (f_1, \dots, f_n)\colon (X, 0) \to (\mathbb{R}^n, 0) \quad \text{and} \quad J = (g_1, \dots, g_m)\colon (X, 0) \to (\mathbb{R}^m, 0)$$

are bilipschitz equivalent. It suffices to prove that the outer metric for the embedding $(f_1, \dots, f_n, g_1, \dots, g_m)$ is bilipschitz equivalent to the metric d_I. By induction, we just have to prove that for any $g \in \mathcal{M}$, the metric $d_{I'}$ associated with the embedding $I' = (f_1, \dots, f_n, g)\colon (X, 0) \to (\mathbb{R}^{n+1}, 0)$ is bilipschitz equivalent to d_I.

Since g is in the ideal $\mathcal{M}$, it may be expressed as $G(f_1, \dots, f_n)$ where $G\colon (\mathbb{R}^n, 0) \to (\mathbb{R}, 0)$ is real analytic. Let Γ be the graph of the function $G(x_1, \dots, x_n)$ in $(\mathbb{R}^n, 0) \times \mathbb{R}$.

It is defined over a neighbourhood of 0 in $\mathbb{R}^n$. The projection $\pi\colon \Gamma \to (\mathbb{R}^n, 0)$ is bilipschitz over any compact neighbourhood of 0 in $\mathbb{R}^n$ on which it is defined. We have $I'(X,0) \subset \Gamma \subset (\mathbb{R}^n, 0) \times \mathbb{R}$, so $\pi|_{I'(X,0)}\colon I'(X,0) \to I(X,0)$ is bilipschitz for the outer metrics $d_{I'}$ and d_I.

2 The Lipschitz geometry of a complex curve singularity

2.1 Complex curves have trivial inner Lipschitz geometry

Let $X \subset \mathbb{C}^2$ be the complex cusp with equation $y^2 - x^3 = 0$. Let $t \in \mathbb{R}$ and consider the two points $p_1(t) = (t^2, t^3)$ and $p_2(t) = (t^2, -t^3)$ on X. Since these two points are on two distinct strands of the braid $X \cap (S^1_{|t|} \times \mathbb{C})$, it is easy to see that the shortest path in X from $p_1(t)$ to $p_2(t)$ passes through the origin and that $d_i(p_1(t), p_2(t)) = \Theta(t)$. This suggests that $(X, 0)$ is locally inner bilipschitz homeomorphic to the cone over its link. This means that the inner Lipschitz geometry tells one no more than the topological type, i.e., the number of connected components of the link (which are circles), and is therefore uninteresting. The aim of this section is to prove this for any complex curve.

Definition 2.1. An analytic germ $(X, 0)$ is **metrically conical** if it is inner Lipschitz homeomorphic to the straight cone over its link.

In this paper, a **complex curve germ** or **complex curve singularity** will mean a germ of reduced complex analytic space of dimension 1.

Proposition 2.2. *Any complex space curve germ $(C, 0) \subset (\mathbb{C}^N, 0)$ is metrically conical.*

Proof. Take a linear projection $p\colon \mathbb{C}^N \to \mathbb{C}$ which is generic for the curve $(C, 0)$ (*i.e.*, its kernel contains no tangent line of C at 0) and let $\pi := p|_C$, which is a branched cover of germs. Let $D_\epsilon = \{z \in \mathbb{C} : |z| \leq \epsilon\}$ with ϵ small, and let E_ϵ be the part of C which branched covers D_ϵ. Since π is holomorphic away from 0 we have a local Lipschitz constant $K(x)$ at each point $x \in C \setminus \{0\}$ given by the absolute value of the derivative map of π at x. On each branch γ of C this $K(x)$ extends continuously over 0 by taking for $K(0)$ the absolute value of the restriction $p\,|_{T_0\gamma}\colon T_0\gamma \to \mathbb{C}$ where $T_0\gamma$ denotes the tangent cone to γ at 0. So the infimum and supremum K^- and K^+ of $K(x)$ on $E_\epsilon \setminus \{0\}$ are defined and positive. For any arc γ in E_ϵ which is smooth except where it passes through 0 we have $K^-\ell(\gamma) \leq \ell'(\gamma) \leq K^+\ell(\gamma)$, where ℓ respectively ℓ' represent arc length using inner metric on e_ϵ respectively the metric lifted from B_ϵ. Since E_ϵ with the latter metric is strictly conical, we are done.

2.2 The outer Lipschitz geometry of a complex curve

Let $\mathbf{G}(n-2,\mathbb{C}^n)$ be the Grassmanian of $(n-2)$-planes in $\mathbb{C}^n$.

Let $\mathcal{D} \in \mathbf{G}(n-2,\mathbb{C}^n)$ and let $\ell_{\mathcal{D}}\colon \mathbb{C}^n \to \mathbb{C}^2$ be the linear projection with kernel $\mathcal{D}$. Suppose $(C,0) \subset (\mathbb{C}^n,0)$ is a complex curve germ. There exists an open dense subset Ω_C of $\mathbf{G}(n-2,\mathbb{C}^n)$ such that for $\mathcal{D} \in \Omega_C$, $\mathcal{D}$ contains no limit of secant lines to the curve C ([Tei82, pp. 354]).

Definition 2.3. The projection $\ell_{\mathcal{D}}$ is said to be **generic for** C if $\mathcal{D} \in \Omega_C$.

In the sequel, we will use extensively the following result

Theorem 2.4 ([Tei82, pp. 352-354]). *If $\ell_{\mathcal{D}}$ is a generic projection for C, then the restriction $\ell_{\mathcal{D}}|_C\colon C \to \ell_{\mathcal{D}}(C)$ is a bilipschitz homeomorphism for the outer metric.*

As a consequence of Theorem 2.4, in order to understand Lipschitz geometry of curve germs, it suffices to understand Lipschitz geometry of plane curve germs.

Let us start with an example.

Example 2.5. Consider the plane curve germ $(C,0)$ with two branches having Puiseux expansions

$$y = x^{3/2} + x^{13/6}, \quad y = x^{5/2}\,.$$

Its topological type is completely described by the sets of characteristic exponents of the branches: $\{3/2, 13/6\}$ and $\{5/2\}$ and by the contact exponents between the two branches: $3/2$. Those data are summarized in the Eggers-Wall tree of the curve germ (see [Wal04, GBGPPP19]), or equivalently, in what we will call the **carrousel tree** (see the proof of Lemma 2.8 and Figure 2), which is exactly the Kuo-Lu tree defined in [KL77] but with the horizontal bars contracted to points.

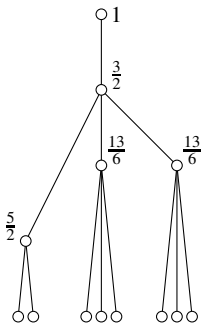


Fig. 2: The carrousel tree

Now, for small $t \in \mathbb{R}^+$, consider the intersection $C \cap \{x = t\}$. This gives 8 points $p_i(t), i = 1\ldots,8$ and then, varying t, this gives 8 real semi-analytic arcs $p_i\colon [0,1) \to X$ such that $p_i(0) = 0$ and $\|p_i(t)\| = \Theta(t)$.

Figure 3 gives pictures of sections of C with complex lines $x = 0.1, 0.05, 0.025$ and 0. The central two-points set corresponds to the branch $y = x^{5/2}$ while the two lateral three-points sets correspond to the other branch.

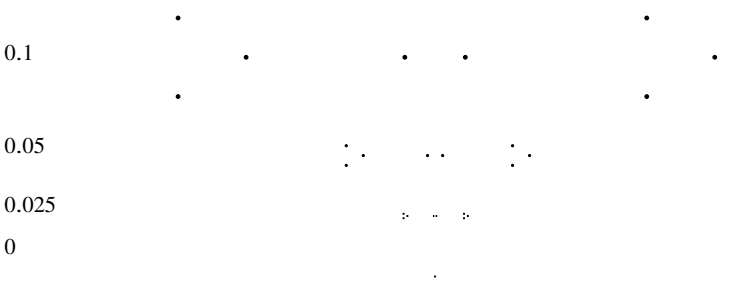


Fig. 3: Sections of C

It is easy to see on this example that for each pair (i, j) with $i \neq j$, we have $d_o(p_i(t), p_j(t)) = \Theta(t^{q(i,j)})$ where $q(i, j) \in \mathbb{Q}^+$ and that the set of such $q(i, j)$'s is exactly the set of essential exponents $\{3/2, 13/6, 5/2\}$. This shows that one can recover the essential exponents by measuring the outer distance between points of C.

More generally, we will show that we can actually recover the carrousel tree by measuring outer distances on X even after a bilipschitz change of the metric. Conversely, the outer Lipschitz geometry of a plane curve is determined by its embedded topological type. This gives the complete classification of the outer geometry of complex plane curve germs:

Theorem 2.6. *Let $(E_1, 0) \subset (\mathbb{C}^2, 0)$ and $(E_2, 0) \subset (\mathbb{C}^2, 0)$ be two germs of complex curves. The following are equivalent:*

1. *$(E_1, 0)$ and $(E_2, 0)$ have same outer Lipschitz geometry.*
2. *there is a meromorphic germ $\phi\colon (E_1, 0) \to (E_2, 0)$ which is a bilipschitz homeomorphism for the outer metric;*
3. *$(E_1, 0)$ and $(E_2, 0)$ have the same embedded topological type;*
4. *there is a bilipschitz homeomorphism of germs $h\colon (\mathbb{C}^2, 0) \to (\mathbb{C}^2, 0)$ with $h(E_1) = E_2$.*

As a corollary of Theorem 2.4 and Theorem 2.6, we obtain:

Corollary 2.7. *The outer Lipschitz geometry of a curve germ $(C, 0) \subset (\mathbb{C}^N, 0)$ determines and is determined by the embedded topological type of any generic linear projection $(\ell(C), 0) \subset (\mathbb{C}^2, 0)$.*

The equivalence of (1), (3) and (4) of Theorem 2.6 is proved in [NP14]. The equivalence of (2) and (3) was first proved by Pham and Teissier [PT69] by developing the theory of Lipschitz saturation and revisited by Fernandes in [Fer03]. In the present

lecture notes, we will give the proof of (1) ⇒ (3), since it is based on the so-called *bubble trick* argument which can be considered as a prototype for exploring Lipschitz geometry of singular spaces in various settings. Another more sophisticated bubble trick argument is developed in [NP12] to study Lipschitz geometry of surface germs (namely in the proof of Theorem 4.36).

Proof (of (1) ⇒ (3) *of Theorem 2.6).* We want to prove that the embedded topological type of a plane curve germ $(C,0) \subset (\mathbb{C}^2,0)$ is determined by the outer Lipschitz geometry of $(C,0)$.

We first prove this using the analytic structure and the outer metric on $(C,0)$. The proof is close to Fernandes' approach in [Fer03]. We then modify the proof to make it purely topological and to allow a bilipschitz change of the metric.

The tangent cone to C at 0 is a union of lines $L^{(j)}$, $j = 1,\dots,m$, and by choosing our coordinates we can assume they are all transverse to the y-axis.

There is $\epsilon_0 > 0$ such that for every $\epsilon \in (0,\epsilon_0]$, the curve C meets transversely the set

$$T_\epsilon := \{(x,y) \in \mathbb{C}^2 : |x| = \epsilon\}\,.$$

Let M be the multiplicity of C. The hypothesis of transversality to the y-axis means that the lines $x = t$ for $t \in (0,\epsilon_0]$ intersect C in M points $p_1(t),\dots,p_M(t)$. Those points depend continuously on t. Denote by $[M]$ the set $\{1,2,\dots,M\}$. For each $j,k \in [M]$ with $j < k$, the distance $d(p_j(t),p_k(t))$ has the form $O(t^{q(j,k)})$, where $q(j,k) = q(k,j) \in \mathbb{Q} \cap [1,+\infty)$ is either a characteristic Puiseux exponent for a branch of the plane curve C or a coincidence exponent between two branches of C in the sense of e.g., [TMW89]. We call such exponents **essential**.

For $j \in [M]$, define $q(j,j) = \infty$.

Lemma 2.8. *The map $q\colon [M]\times[M] \to \mathbb{Q}\cup\{\infty\}$, $(j,k) \mapsto q(j,k)$, determines the embedded topology of C.*

Proof. To prove the lemma we will construct from q the so-called *carrousel tree*. Then, we will show that it encodes the same data as the Eggers tree. This implies that it determines the embedded topology of C.

The $q(j,k)$ have the property that $q(j,l) \geq min(q(j,k),q(k,l))$ for any triple j,k,l. So for any $q \in \mathbb{Q}\cup\{\infty\}$, $q > 0$, the binary relation on the set $[M]$ defined by $j \sim_q k \Leftrightarrow q(j,k) \geq q$ is an equivalence relation.

Name the elements of the set $q([M]\times[M])\cup\{1\}$ in decreasing order of size: $\infty = q_0 > q_1 > q_2 > \cdots > q_s = 1$. For each $i = 0,\dots,s$ let $G_{i,1},\dots,G_{i,M_i}$ be the equivalence classes for the relation $\sim_{q_i}$. So $M_0 = M$ and the sets $G_{0,j}$ are singletons while $M_s = 1$ and $G_{s,1} = [M]$. We form a tree with these equivalence classes $G_{i,j}$ as vertices, and edges given by inclusion relations: the singleton sets $G_{0,j}$ are the leaves and there is an edge between $G_{i,j}$ and $G_{i+1,k}$ if $G_{i,j} \subseteq G_{i+1,k}$. The vertex $G_{s,1}$ is the root of this tree. We weight each vertex with its corresponding q_i.

The **carrousel tree** is the tree obtained from this tree by suppressing valence 2 vertices (i.e., vertices with exactly two incident edges): we remove each such vertex and amalgamate its two adjacent edges into one edge. We follow the computer

science convention of drawing the tree with its root vertex at the top, descending to its leaves at the bottom (see Figure 2).

At any non-leaf vertex v of the carrousel tree we have a weight q_v, $1 \leq q_v \leq q_1$, which is one of the q_i's. We write it as m_v/n_v, where n_v is the lcm of the denominators of the q-weights at the vertices on the path from v up to the root vertex. If v' is the adjacent vertex above v along this path, we put $r_v = n_v/n_{v'}$ and $s_v = n_v(q_v - q_{v'})$. At each vertex v the subtrees cut off below v consist of groups of r_v isomorphic trees, with possibly one additional tree. We label the top of the edge connecting to this additional tree at v, if it exists, with the number r_v, and then delete all but one from each group of r_v isomorphic trees below v. We do this for each non-leaf vertex of the carrousel tree. The resulting tree, with the q_v labels at vertices and the extra label on a downward edge at some vertices is easily recognized as a mild modification of the Eggers tree: there is a natural action of the Galois group whose quotient is the Eggers tree.

As already noted, this reconstruction of the embedded topology involved the complex structure and the outer metric. We must show that we can reconstruct it without using the complex structure, even after applying a bilipschitz change to the outer metric. We will use what we call a **bubble trick**.

Recall that the tangent cone of C is a union of lines $L^{(j)}$. We denote by $C^{(j)}$ the part of C tangent to the line $L^{(j)}$. It suffices to recover the topology of each $C^{(j)}$ independently, since the $C^{(j)}$'s are distinguished by the fact that the distance between any two of them outside a ball of radius ϵ around 0 is $\Theta(\epsilon)$, even after bilipschitz change of the metric. We therefore assume from now on that the tangent cone of C is a single complex line.

We now arrive at a crucial moment of the proof and of the paper.

The bubble trick. The points $p_1(t), \ldots, p_M(t)$ which we used in order to find the numbers $q(j,k)$ were obtained by intersecting C with the line $x = t$. The arc $p_1(t)$, $t \in [0, \epsilon_0]$ satisfies $d(0, p_1(t)) = \Theta(t)$. Moreover, the other points $p_2(t), \ldots, p_M(t)$ are in the transverse disk of radius rt centered at $p_1(t)$ in the plane $x = t$. Here r can be as small as we like, so long as ϵ_0 is then chosen sufficiently small.

Instead of a transverse disk of radius rt, we can use a ball $B(p_1(t), rt)$ of radius rt centered at $p_1(t)$. This ball $B(p_1(t), rt)$ intersects C in M disks $D_1(t), \ldots, D_M(t)$, and we have $d(D_j(t), D_k(t)) = \Theta(t^{q(j,k)})$, so we still recover the numbers $q(j,k)$. In fact, the ball in the outer metric on C of radius rt around $p_1(t)$ is $B_C(p_1(t), rt) := C \cap B(p_1(t), rt)$, which consists of these M disks $D_1(t), \ldots, D_M(t)$.

We now replace the arc $p_1(t)$ by any continuous arc $p_1'(t)$ on C with the property that $d(0, p_1'(t)) = \Theta(t)$. If r is sufficiently small it is still true that $B_C(p_1'(t), rt)$ consists of M disks $D_1'(t), \ldots, D_M'(t)$ with $d\big(D_j'(t), D_k'(t)\big) = \Theta(t^{q(j,k)})$. So at this point, we have gotten rid of the dependence on analytic structure in discovering the topology, but not yet of the dependence on the outer geometry.

Let now d' be a metric on C such that the identity map is a K-bilipschitz homeomorphism in a neighbourhood of the origin. We work inside this neighbourhood, taking t, ϵ_0 and r sufficiently small. $B'(p, \eta)$ will denote the ball in C for the metric d' centered at $p \in C$ with radius $\eta \geq 0$.

The bilipschitz change of the metric may disintegrate the balls in many connected components, as sketched on Figure 4, where the round ball $B_C(p'_1(t), rt)$ has 3 components (3 is the mulitplicity of C), while $B'(p'_1(t), rt)$ has 6 components (for clarity of the picture, we draw the ball $B'(p'_1(t), rt)$ as if the distance d' were induced by an ambient metric, but this is not the case in general).

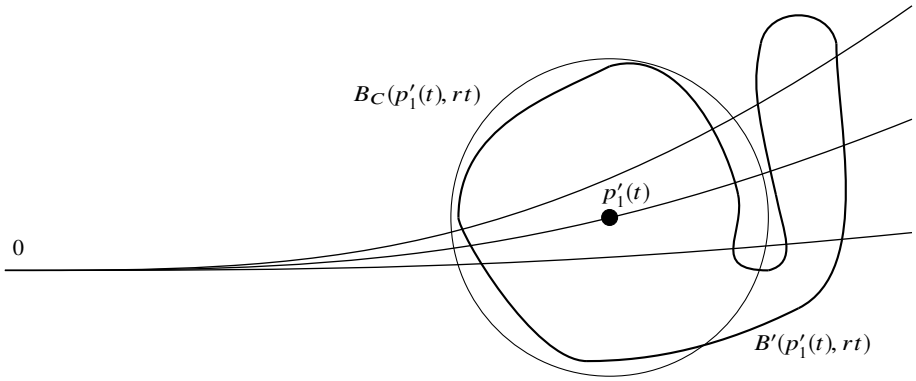


Fig. 4: Change of the metric

If we try to perform the same argument as before using the balls $B'(p'_1(t), rt)$ instead of $B_C(p'_1(t), rt)$, we get a problem since $B'(p'_1(t), rt)$ may have many irrelevant components and we can no longer simply use distance between connected components. To resolve this, we consider the two balls $B'_1(t) = B'(p'_1(t), \frac{rt}{K^3})$ and $B'_2(t) = B'(p'_1(t), \frac{rt}{K})$, we have the inclusions:

$$B_C\big(p'_1(t), \frac{rt}{K^4}\big) \subset B'_1(t) \subset B_C\big(p'_1(t), \frac{rt}{K^2}\big) \subset B'_2(t) \subset B_C\big(p'_1(t), rt\big)$$

Using these inclusions, we obtain that only M components of $B'_1(t)$ intersect $B'_2(t)$ and that naming these components $D'_1(t), \dots, D'_M(t)$ again, we still have $d(D'_j(t), D'_k(t)) = \Theta(t^{q(j,k)})$ so the $q(j,k)$ are determined as before (prove this as an exercise). See Figure 5 for a schematic picture of the situation (again, for clarity of the picture, we draw the balls $B'_1(t)$ and $B'_2(t)$ as if the distance d' were induced by an ambient metric, but this is not the case in general).

2.3 The bubble trick with jumps

The “bubble trick" introduced in the proof of Theorem 2.6 is a powerful tool to capture invariants of Lipschitz geometry of a complex curve germ. However, this first version of the bubble trick is not well adapted to explore the outer Lipschitz geometry of a singular space of dimension ≥ 2 for the following reason. In the

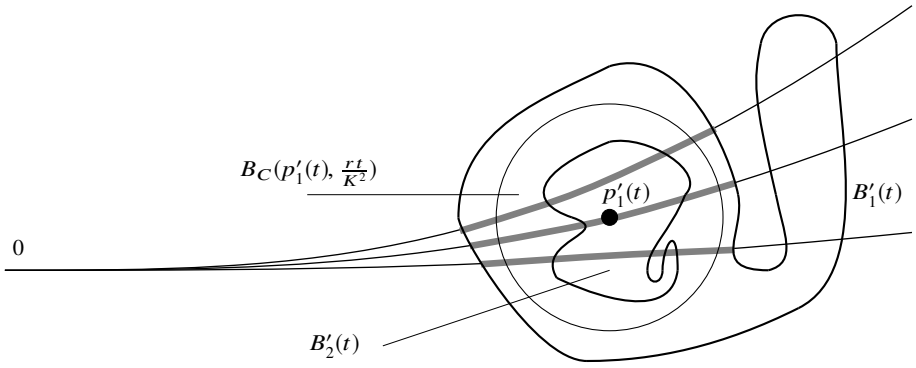


Fig. 5: The bubble trick

case of a plane curve germ $(C, 0)$, the bubble trick is based on the fact that the distance orders between points of $\ell^{-1}(t) \cap C$ with respect to $t \in \mathbb{R}$ are Lipschitz invariants, where $\ell\colon (C, 0) \to (\mathbb{C}, 0)$ denotes a generic projection of the curve germ. Now, assume that $(X, 0)$ is a complex surface germ with multiplicity $m \geq 2$ (so it has a singularity at 0), and consider a generic projection $\ell\colon (X, 0) \to (\mathbb{C}^2, 0)$. Then the critical locus of ℓ is a curve germ $(\Pi_\ell, 0) \subset (X, 0)$ called the **polar curve**, and its image $\Delta_\ell = \ell(\Pi_\ell)$ is a curve germ $(\Delta_\ell, 0) \subset (\mathbb{C}^2, 0)$ called the **discriminant curve** of ℓ. Let $x \in \mathbb{C}^2 \setminus \{0\}$. The number of points in $\ell^{-1}(x) \cap C$ depends on x: it equals $m - 1$ if $x \in \Delta_\ell$, where m denotes the multiplicity of $(X, 0)$, and m otherwise. Moreover, consider a semialgebraic real arc germ $p\colon t \in [0, \eta) \mapsto p(t) \in \mathbb{C}^2$ such that $\|p(t)\| = |t|$ and $\forall t \neq 0, p(t) \notin \Delta_\ell$; then the distance orders between the m points $p_1(t), \ldots, p_m(t)$ of $\ell^{-1}(p(t))$ will depend on the position of the arc $p(t)$ with respect to the curve Δ_ℓ. So the situation is much more complicated, even in dimension 2.

In [NP14], we use an adapted version of the bubble trick which enables us to explore the outer Lipschitz geometry of a complex surface $(X, 0)$. We call it the **bubble trick with jumps**. Roughly speaking, it consists in using horns

$$\mathcal{H}(p(t), r|t|^q) = \bigcup_{t \in [0,1)} B((p(t), r|t|^q),$$

where $B(x, a)$ denotes the ball in X with center x and radius a and where $p(t)$ is a real arc on $(X, 0)$ such that $||p(t)|| = \Theta(t)$ and $r \in]0, +\infty[$, and in exploring "jumps" in the topology of $\mathcal{H}(p(t), a|t|^q)$ when q varies from $+\infty$ to 1, for example, jumps of the number of connected components of $\mathcal{H}(p(t), r|t|^q) \setminus \{0\}$.

In order to give a flavour of this bubble trick with jumps, we will perform it on a plane curve germ, giving an alternative proof of the implication (1) $\Rightarrow$ (3) of Theorem 2.6.

The bubble trick with jumps.

We use again the notations of the version 1 of the bubble trick from the proof of Theorem 2.6. Let $(C,0)$ be a plane curve germ with multiplicity M and with s branches $C_1,\dots,C_s$. Let $p_1'(t)$ be a continuous arc on C_1 with the property that $d(0,p_1'(t)) = \Theta(t)$. Let us order the numbers $q(1,k), k = 2,\dots,M$ in decreasing order:

$$1 \leq q(1,M) < q(1,M-1) < \cdots < q(1,2) < q(1,1) = \infty.$$

Let us consider the horns $\mathcal{H}_{q,r} = \mathcal{H}(p_1'(t), r|t|^q)$ with $q \in [1,+\infty[$.

For $q >> 1$ and small $\epsilon > 0$, the number of connected components of $B(0,\epsilon) \cap \big(\mathcal{H}_{q,r} \setminus \{0\}\big)$ equals 1. Now, let us decrease q. For every $\eta > 0$ small enough, the number of connected components of $\mathcal{H}_{q_1,2+\eta} \setminus \{0\}$ equals 1, while the number of connected components of $\mathcal{H}_{q_1,2-\eta} \setminus \{0\}$ is > 2. Decreasing q, we have a jump in the number of connected components exactly when passing one of the rational numbers $q(1,k)$. So this enables one to recover all the characteristic exponents of C_1 and its contact exponents with the other branches of C. We can do the same for a real arc $p_i'(t)$ in each branch C_i of $(C,0)$ and this will recover the integers $q(i,k)$ for $k = 1,\dots,M$. We then reconstruct the function $q\colon [M]\times[M] \to \mathbb{Q}_{\geq 1}$ which characterizes the embedded topology of $(C,0)$, or equivalently the carrousel tree of $(C,0)$.

Moreover, the same jumps appear when one uses instead horns

$$\mathcal{H}'(p'(t), r|t|^q) = \bigcup_{t\in[0,1)} B'((p'(t), r|t|^q),$$

where B' denotes balls with respect to a metric d' which is bilipschitz equivalent to the initial outer metric. Indeed, if K is the bilipschitz constant of such a bilipschitz change, then we have the inclusions

$$\mathcal{H}\big(p'(t), \frac{rt}{K^4}\big) \subset \mathcal{H}'\big(p'(t), \frac{rt}{K^3}\big) \subset \mathcal{H}\big(p'(t), \frac{rt}{K^2}\big)$$
$$\subset \mathcal{H}'\big(p'(t), \frac{rt}{K^3}\big) \subset \mathcal{H}\big(p'(t), rt\big).$$

Then the same argument as in the version 1 of the bubble trick shows that for q fixed and different from $q(1,k), k = 2,\dots,M$, the numbers of connected components of $B(0,\epsilon) \cap \big(\mathcal{H}_{q,r} \setminus \{0\}\big)$ and $B(0,\epsilon) \cap \big(\mathcal{H'}_{q,r} \setminus \{0\}\big)$ are equal.

Example 2.9. Consider again the plane curve singularity with two branches of Example 2.5 given by the Puiseux series:

$$C_1 : \quad y = x^{3/2} + x^{13/6}, \qquad C_2 : \quad y = x^{5/2}\,.$$

Consider first an arc $p_1'(t)$ inside C_1 parametrized by $x = t \in [0,1)$. Then $p_1'(t)$ corresponds to one of the two extremities of the carrousel tree of Figure 2 whose neighbour vertex is weighted by $5/2$. Figure 6 represents the intersection of the horn $\mathcal{H}_{q,r}$ with the line $\{x = t\}$ for different values of $q \in [1,+\infty[$ and for $t \in \mathbb{C}^*$ of sufficiently small absolute value. This shows two jumps: a first jump at $q = 5/2$,

which says that $5/2$ is a characteristic exponent of a branch since $p_1'(t)$ and the new point appearing in the intersection belong to the same connected component C_1 of $C \setminus \{0\}$, while the second jump at $3/2$ says that $3/2$ is the contact exponent of C_1 with the other component since the new points appearing at $q = 3/2 - \eta$ belong to C_2.

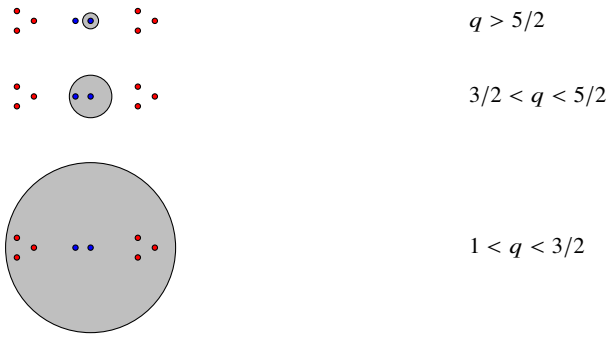


Fig. 6: Sections of C associated to the arc $p_1'(t)$

This first exploration enables one to construct the left part of the carrousel tree of C shown on Figure 7, i.e., the one corresponding to the carrousel tree of C_1.

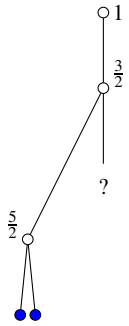


Fig. 7: Partial carrousel tree associated to the arc $p_1'(t)$

To complete the picture, we now consider an arc $p_2'(t)$ inside C_2 corresponding to a component of $C_2 \cap \{x = t\}$. This means that $p_2'(t)$ corresponds to one of the 6 extremities of the carrousel tree of Figure 2 whose neighbour vertex is weighted by $13/6$. Figure 8 represents the jumps for the horns $\mathcal{H}_{q,r,}$ centered on $p_2'(t)$. This shows two jumps: a first jump at $q = 13/6$, which says that $13/6$ is a characteristic exponent of C_2, then a second jump at $3/2$ corresponding to the contact exponent of C_1 and C_2.

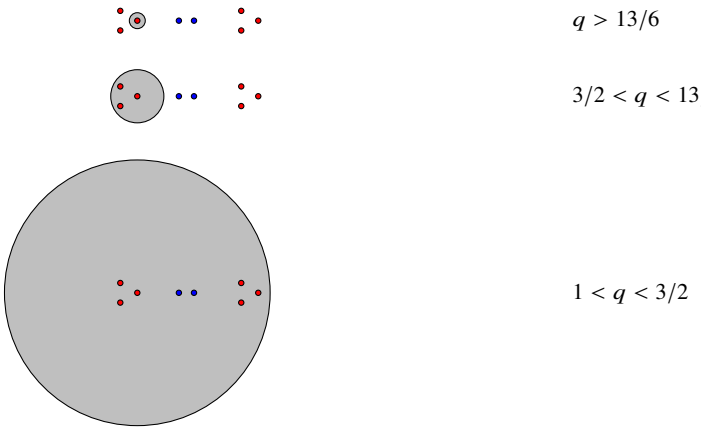


Fig. 8: Sections of C associated to the arc $p_2'(t)$

This exploration of C_2 enables one to construct the right part of the carrousel tree of C shown on Figure 9, i.e., the one corresponding to the carrousel tree of C_2.

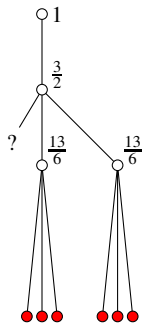


Fig. 9: Partial carrousel tree associated to the arc $p_2'(t)$

Merging the two partial carrousel trees above, we obtain the carrousel tree of Figure 2, recovering the embedded topology of $(C, 0)$.

3 The thick-thin decomposition of a surface singularity

3.1 Fast loops as obstructions to metric conicalness

We know that every complex curve germ $(C,0) \subset (\mathbb{C}^N,0)$ is metrically conical for the inner geometry (Proposition 2.2). This is no longer true in higher dimensions. The first example of a non-metrically-conical complex analytic germ (X,0) appeared in [BF08]: for $k \geq 2$, the surface singularity $A_k : x^2 + y^2 + z^{k+1} = 0$ is not metrically conical for the inner metric[1]. The examples in [BFN08, BFN09, BFN10] then suggested that failure of metric conicalness is common. For example, among ADE singularities of surfaces, only A_1 and D_4 are metrically conical (Exercise 3.22). In [BFN10] it is also shown that the inner Lipschitz geometry of a singularity may not be determined by its topological type.

A complete classification of the Lipschitz inner geometry of normal complex surfaces is presented in [BNP14]. It is based on the existence of the so-called thick-thin decomposition of the surface into two semi-algebraic sets. The aim of Sections 3.1 to 3.3 is to describe this decomposition.

The simplest obstruction to the metric conicalness of a germ $(X,0)$ is the existence of *fast loops* (see Definition 3.2 below).

Let p and q be two pairwise coprime positive integers such that $p \geq q$. Set $\beta = \frac{p}{q}$. The prototype of a fast loop is the **β-horn**, which is the following semi-algebraic surface in $\mathbb{R}^3$:

$$\mathcal{H}_\beta = \{(x,y,z) \in \mathbb{R}^2 \times \mathbb{R}^+ : (x^2+y^2)^q = (z^2)^p\}.$$

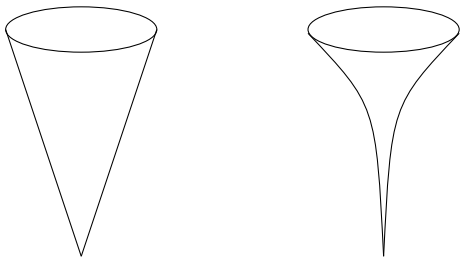


Fig. 10: The β-horns $\mathcal{H}_\beta$

[1] Notice that in the real algebraic setting, it is easy to construct germs with dimension ≥ 3 which are not metrically conical for the inner geometry. For example a 3-dimensional horn-shaped germ $(X,0)$ whose link $X^{(\epsilon)}$ is a 2-torus with diameter $\Theta(\epsilon^2)$

Exercise 3.1. Show that $\mathcal{H}_\beta$ is inner bilipschitz homeomorphic to $\mathcal{H}_{\beta'}$ if and only if $\beta = \beta'$. [2]

$\mathcal{H}_1$ is a straight cone, so it is metrically conical. As a consequence of Exercise 3.1, we obtain that for $\beta > 1$, $\mathcal{H}_\beta$ is not metrically conical. For $t > 0$, set $\gamma_t = \mathcal{H}_\beta \cap \{z = t\}$. When $\beta > 1$, the family of curves $(\gamma_t)_{t>0}$ is a *fast loop* inside $\mathcal{H}_\beta$. More generally:

Definition 3.2. Let $(X, 0) \subset (\mathbb{R}^n, 0)$ be a semianalytic germ. A **fast loop** in $(X, 0)$ is a continuous family of loops $\{\gamma_\epsilon : S^1 \to X^{(\epsilon)}\}_{0<\epsilon\leq\epsilon_0}$ such that:

1. γ_ϵ is essential (i.e., homotopically non trivial) in the link $X^{(\epsilon)} = X \cap S_\epsilon$;
2. there exists $q > 1$ such that

$$\lim_{\epsilon\to 0} \frac{\text{length}(\gamma_\epsilon)}{\epsilon^q} = 0.$$

In the next section, we will define what we call **the thick-thin decomposition of a normal surface germ** $(X, 0)$. It consists in decomposing $(X, 0)$ as a union of two semi-algebraic sets $(X, 0) = (Y, 0) \bigcup (Z, 0)$ where $(Z, 0)$ is *thin* (Definition 3.5) and where $(Y, 0)$ is *thick* (Definition 3.10). The thin part $(Z, 0)$ will contain all the fast loops of $(X, 0)$ inside a Milnor ball with radius ϵ_0. The thick part $(Y, 0)$ is the closure of the complement of the thin part and has the property that it contains a maximal metrically conical set. This enables one to characterize the germs $(X, 0)$ which are metrically conical:

Theorem 3.3. *[BNP14, Theorem 7.5, Corollary 1.8] Let $(X, 0)$ be a normal complex surface and let*

$$(X, 0) = (X_{thick}, 0) \bigcup (X_{thin}, 0)$$

be its thick-thin decomposition.

Then $(X, 0)$ is metrically conical if and only if $X_{thin} = \emptyset$, so $(X, 0) = (X_{thick}, 0)$.

3.2 Thick-thin decomposition

Definition 3.4. Let $(Z, 0) \subset (\mathbb{R}^n, 0)$ be a semi-algebraic germ. The *tangent cone* of $(Z, 0)$ is the set T_0Z of vectors $v \in \mathbb{R}^n$ such that there exists a sequence of points (x_k) in $Z \setminus \{0\}$ tending to 0 and a sequence of positive real numbers (t_k) such that

$$\lim_{k\to\infty} \frac{1}{t_k} x_k = v.$$

Definition 3.5. A semi-algebraic germ $(Z, 0) \subset (\mathbb{R}^n, 0)$ of pure dimension is **thin** if the dimension of its tangent cone T_0X at 0 satisfies $\dim(T_0Z) < \dim(Z)$.

[2] *hint:* the length of the family of curves $C_t = \mathcal{H}_\beta \cap \{z = t\}$ is a $\Theta(t^\beta)$ and this is invariant by a bilipschitz change of the metric. Show that such a family of curves cannot exist in $\mathcal{H}_{\beta'}$ if $\beta' \neq \beta$.

Example 3.6. For every $\beta > 1$, the β-horn $\mathcal{H}_\beta$ is thin since $\dim(\mathcal{H}_\beta) = 2$ while $T_0\mathcal{H}_\beta$ is a half-line. On the other hand, $\mathcal{H}_1$ is not thin.

Example 3.7. Let $\lambda \in \mathbb{C}^*$ and denote by C_λ the plane curve with Puiseux parametrization $y = \lambda x^{5/3}$. Let $a, b \in \mathbb{R}$ such that $0 < a < b$. Consider the semi-algebraic germ $(Z, 0) \subset (\mathbb{C}^2, 0)$ defined by $Z = \bigcup_{a \leq |\lambda| \leq b} C_\lambda$. The tangent cone T_0Z is the complex line $y = 0$, while Z is 4-dimensional, so $(Z, 0)$ is thin.

Let $Z^{(\epsilon)}$ be the intersection of Z with the boundary of the bidisc $\{|x| \leq \epsilon\} \times \{|y| \leq \epsilon\}$. By [Dur83], one obtains, up to homeomorphism (or diffeomorphism in a stratified sense), the same link $Z^{(\epsilon)}$ as when intersecting with a round sphere. When $\epsilon > 0$ is small enough, $Z^{(\epsilon)} \subset \{|x| = \epsilon\} \times \{|y| \leq \epsilon\}$ and the projection $Z^{(\epsilon)} \to S^1_\epsilon$ defined by $(x, y) \to x$ is a locally trivial fibration whose fibers are the flat annuli $A_t = Z \cap \{x = t\}, |t| = \epsilon$, and the lengths of the boundary components of A_t are $\Theta(\epsilon^{5/3})$.

Notice that Z can be described through a resolution as follows. Let $\sigma : Y \to \mathbb{C}^2$ be the minimal embedded resolution of the curve $E_1 : y = x^{5/3}$. It decomposes into four successive blow-ups of points. Denote $E_1, \ldots, E_4$ the corresponding components of the exceptional divisor $\sigma^{-1}(0)$ indexed by their order of creation. Then σ is a simultaneous resolution of the curves C_λ. Therefore, the strict transform of Z by σ is a neighbourhood of E_4 minus neighbourhoods of the intersecting points $E_4 \cap E_2$ and $E_4 \cap E_3$ as pictured in Figure 11. The tree T on the left is the dual tree of σ. Its vertices are weighted by the self-intersections E_i^2 and the arrow represents the strict transform of C_1.

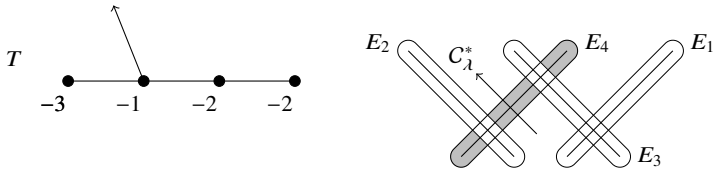


Fig. 11: The strict transform of Z by σ

Definition 3.8. Let $1 < q \in \mathbb{Q}$. A **q-horn neighbourhood** of a semi-algebraic germ $(A, 0) \subset (\mathbb{R}^N, 0)$ is a set of the form $\{x \in \mathbb{R}^n \cap B_\epsilon : d(x, A) \leq c|x|^q\}$ for some $c > 0$, where d denotes the Euclidean metric.

The following proposition helps picture "thinness"

Proposition 3.9. *[BNP14, Proposition 1.3] Any thin semi-algebraic germ $(Z, 0) \subset (\mathbb{R}^N, 0)$ is contained in some q-horn neighbourhood of its tangent cone T_0Z.*

We will now define thick semi-algebraic sets. The definition is built on the following observation. Let $(X, 0) \subset (\mathbb{R}^n, 0)$ be a real algebraic germ; we would like to decompose $(X, 0)$ into two semialgebraic sets $(A, 0)$ and $(B, 0)$ glued along their

boundary germs, where $(A, 0)$ is thin and $(B, 0)$ is metrically conical. But try to glue a thin germ $(A, 0)$ with a metrically conical germ $(B, 0)$ so that they intersect only along their boundary germs.... It is not possible! There would be a hole between them (see Figure 12). So we have to replace $(B, 0)$ by something else than conical.

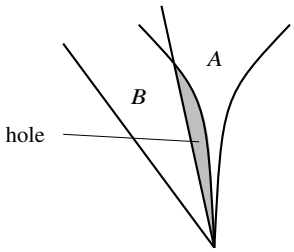


Fig. 12: Trying to glue a thin germ with a metrically conical germ

"Thick" is a generalization of "metrically conical." Roughly speaking, a thick algebraic set is obtained by slightly inflating a metrically conical set in order that it can interface along its boundary with thin parts. The precise definition is as follows:

Definition 3.10. Let $B_\epsilon \subset \mathbb{R}^N$ denote the ball of radius ϵ centered at the origin, and S_ϵ its boundary. A semi-algebraic germ $(Y, 0) \subset (\mathbb{R}^N, 0)$ is **thick** if there exists $\epsilon_0 > 0$ and $K \geq 1$ such that $Y \cap B_{\epsilon_0}$ is the union of subsets Y_ϵ, $\epsilon \leq \epsilon_0$ which are metrically conical with bilipschitz constant K and satisfy the following properties (see Fig. 1):

1. $Y_\epsilon \subset B_\epsilon$, $Y_\epsilon \cap S_\epsilon = Y \cap S_\epsilon$ and Y_ϵ is metrically conical;
2. For $\epsilon_1 < \epsilon_2$ we have $Y_{\epsilon_2} \cap B_{\epsilon_1} \subset Y_{\epsilon_1}$ and this embedding respects the conical structures. Moreover, the difference $(Y_{\epsilon_1} \cap S_{\epsilon_1}) \setminus (Y_{\epsilon_2} \cap S_{\epsilon_1})$ of the links of these cones is homeomorphic to $\partial(Y_{\epsilon_1} \cap S_{\epsilon_1}) \times [0, 1)$.

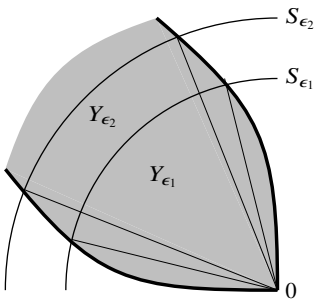


Fig. 13: Thick germ

Clearly, a semi-algebraic germ cannot be both thick and thin.

Example 3.11. The set $Z = \{(x, y, z) \in \mathbb{R}^3 : x^2 + y^2 \leq z^3\}$ gives a thin germ at 0 since it is a 3-dimensional germ whose tangent cone is half the z-axis. The intersection $Z \cap B_\epsilon$ is contained in a closed 3/2-horn neighbourhood of the z-axis. The complement in $\mathbb{R}^3$ of this thin set is thick.

Example 3.12. Consider again the thin germ $(Z, 0) \subset (\mathbb{C}^2, 0)$ of Example 3.7. Then the germ $(Y, 0)$ defined by $Y = \overline{\mathbb{C}^2 \setminus Z}$ is a thick germ. To give an imaged picture of it, fix $\eta > 0$ and consider the conical set $W \subset \mathbb{C}^2$ defined as the union of the complex lines $y = \alpha x$ for $|\alpha| \geq \eta$; then $(Y, 0)$ is obtained by "slighly inflating" W. Notice that the strict transform of Y by the resolution σ introduced in Example 3.7 is a neighbourhood of the union of curves $E_1 \cup E_3$.

For any semi-algebraic germ $(A, 0)$ of $(\mathbb{R}^N, 0)$, we write $A^{(\epsilon)} := A \cap S_\epsilon \subset S_\epsilon$. When ϵ is sufficiently small, $A^{(\epsilon)}$ is the ϵ-link of $(A, 0)$.

Definition 3.13 (Thick-thin decomposition). A **thick-thin decomposition** of the normal complex surface germ $(X, 0)$ is a decomposition of it as a union of semi-algebraic germs of pure dimension 4 called **pieces**:

$$(X, 0) = \bigcup_{i=1}^{r} (Y_i, 0) \cup \bigcup_{j=1}^{s} (Z_j, 0), \tag{1}$$

such that the $Y_i \setminus \{0\}$ and $Z_j \setminus \{0\}$ are connected and:

1. Each Y_i is thick and each Z_j is thin;
2. The $Y_i \setminus \{0\}$ are pairwise disjoint and the $Z_j \setminus \{0\}$ are pairwise disjoint;
3. If ϵ_0 is chosen small enough such that S_ϵ is transverse to each of the germs $(Y_i, 0)$ and $(Z_j, 0)$ for $\epsilon \leq \epsilon_0$, then $X^{(\epsilon)} = \bigcup_{i=1}^{r} Y_i^{(\epsilon)} \cup \bigcup_{j=1}^{s} Z_j^{(\epsilon)}$ decomposes the 3-manifold $X^{(\epsilon)} \subset S_\epsilon$ into connected submanifolds with boundary, glued along their boundary components.

Definition 3.14. A thick-thin decomposition is **minimal** if

1. the tangent cone of its thin part $\bigcup_{j=1}^{s} Z_j$ is contained in the tangent cone of the thin part of any other thick-thin decomposition and
2. the number s of its thin pieces is minimal among thick-thin decompositions satisfying (1).

The following theorem expresses the existence and uniqueness of a minimal thick-thin decomposition of a normal complex surface singularity.

Theorem 3.15. *[BNP14, Section 8] Let $(X, 0)$ be a normal complex surface germ. Then a minimal thick-thin decomposition of $(X, 0)$ exists. For any two minimal thick-thin decompositions of $(X, 0)$, there exists $q > 1$ and a homeomorphism of the germ $(X, 0)$ to itself which takes one decomposition to the other and moves each $x \in X$ by a distance at most $\|x\|^q$.*

3.3 The thick-thin decomposition in a resolution

In this section, we describe explicitly the minimal thick-thin decomposition of a normal complex surface germ $(X,0) \subset (\mathbb{C}^n,0)$ in terms of a suitable resolution of $(X,0)$ as presented in [BNP14, Section 2]. The uniqueness of the minimal thick-thin decomposition is proved in [BNP14, Section 8].

Let $\pi\colon (\widetilde{X},E) \to (X,0)$ be the minimal resolution with the following properties:

1. It is a good resolution, i.e., the irreducible components of the exceptional divisor are smooth and meet transversely, at most two at a time.
2. It factors through the blow-up $e_0\colon X_0 \to X$ of the origin. An irreducible component of the exceptional divisor $\pi^{-1}(0)$ which projects surjectively on an irreducible component of $e_0^{-1}(0)$ will be called an $\mathcal{L}$**-curve**.
3. No two $\mathcal{L}$-curves intersect.

This is achieved by starting with a minimal good resolution, then blowing up to resolve any base points of a general system of hyperplane sections, and finally blowing up any intersection point between $\mathcal{L}$-curves.

Definition 3.16. Let Γ be the resolution graph of the above resolution. A vertex of Γ is called a **node** if it has valence ≥ 3 or represents a curve of genus > 0 or represents an $\mathcal{L}$-curve. If a node represents an $\mathcal{L}$-curve it is called an $\mathcal{L}$*-node* . By the previous paragraph, $\mathcal{L}$-nodes cannot be adjacent to each other. Other types of nodes will be introduced in Definitions 4.23 and 4.31.

A **string** is a connected subgraph of Γ containing no nodes. A **bamboo** is a string ending in a vertex of valence 1.

For each irreducible curve E_ν in E, let $N(E_\nu)$ be a small closed tubular neighborhood of E_ν in $\widetilde{X}$. For any subgraph Γ' of Γ define (see Figure 14):

$$N(\Gamma') := \bigcup_{\nu\in\Gamma'} N(E_\nu) \quad \text{and} \quad \mathcal{N}(\Gamma') := \overline{N(\Gamma) \setminus \bigcup_{\nu\notin\Gamma'} N(E_\nu)}\,.$$

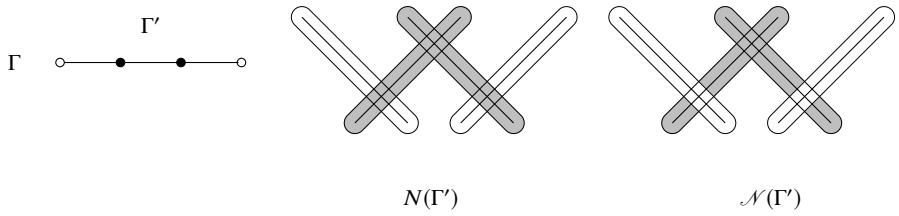


Fig. 14: The sets $N(\Gamma')$ and $\mathcal{N}(\Gamma')$

The subgraphs of Γ resulting by removing the $\mathcal{L}$-nodes and adjacent edges from Γ are called the **Tyurina components** of Γ (following [Spi90, Definition III.3.1]).

Let $\Gamma_1, \dots, \Gamma_s$ denote the Tyurina components of Γ which are not bamboos, and by $\Gamma'_1, \dots, \Gamma'_r$ the maximal connected subgraphs in $\Gamma \setminus \bigcup_{j=1}^{s} \Gamma_j$. Therefore each Γ'_i consists of an $\mathcal{L}$-node and any attached bamboos and strings.

Assume that ϵ_0 is sufficiently small such that $\pi^{-1}(X \cap B_{\epsilon_0})$ is included in $N(\Gamma)$.

For each each $i = 1, \dots, r$, define

$$Y_i := \pi(N(\Gamma'_i)) \cap B_{\epsilon_0},$$

and for each $j = 1, \dots, s$, define

$$Z_j := \pi(\mathcal{N}(\Gamma_j)) \cap B_{\epsilon_0}.$$

Notice that the Y_i are in one-to-one correspondence with the $\mathcal{L}$-nodes.

Theorem 3.17. *[BNP14, Section 2, Proposition 5.1, Proposition 6.1]*

1. *For each $i = 1, \dots, r$, $(Y_i, 0)$ is thick;*
2. *For each $j = 1, \dots, s$, $(Z_j, 0)$ is thin;*
3. *The decomposition $(X, 0) = \bigcup (Z_j, 0) \cup \bigcup (Y_i, 0)$ is a minimal thick-thin decomposition of $(X, 0)$.*

The proof of (2) is easy:

Proof. Choose an embedding $(X, 0) \subset (\mathbb{C}^n, 0)$ and let $e_0 \colon X_0 \to X$ be the blow-up of the origin. If $x \in \mathbb{C}^n \setminus \{0\}$, denote by L_x the class of x in $\mathbb{P}^{n-1}$, so L_x represents the line through 0 and x in $\mathbb{C}^n$. By definition X_0 is the closure in $\mathbb{C}^n \times \mathbb{P}^{n-1}$ of the set $\{(x, L_x) \colon x \in X \setminus \{0\}\}$.

The semi-algebraic set Z_j is of real dimension 4. On the other hand, the strict transform of Z_j by e_0 meets the exceptional divisor $e_0^{-1}(0)$ at a single point (x, L_x), so the tangent cone at 0 to Z_j is the complex line L_x. Therefore $(Z_j, 0)$ is thin.

In the next section, we present the first part of the proof of the thickness of $(Y_i, 0)$, which consists of proving the following intermediate Lemma:

Lemma 3.18. *For each $\mathcal{L}$-node v, the subset $\pi(\mathcal{N}(v))$ of $(X, 0)$ is metrically conical.*

The rest of the proof of Point (1) of Theorem 3.17 is more delicate. In particular, it uses the key Polar Wedge Lemma [BNP14, Proposition 3.4] which is stated later in the present notes (Proposition 4.15) and a geometric decomposition of $(X, 0)$ into standard pieces which is a refinement of the thick-thin decomposition and which leads to the complete classification of the inner Lipschitz geometry of $(X, 0)$ presented in Section 4.4. We refer to [BNP14] for the proofs.

The minimality (3) is proved in [BNP14, Section 8].

We now give several explicit examples of thick-thin decompositions. More examples can be found in [BNP14, Section 15].

Example 3.19. Consider the normal surface singularity $(X, 0) \subset (\mathbb{C}^3, 0)$ with equation $x^2 + y^3 + z^5 = 0$. This is the standard singularity E_8 (see [Dur79]). Its minimal resolution has exceptional divisor a tree of eight $\mathbb{P}^1$ having self intersections -2 and

it factors through the blow-up of the point 0. The dual graph Γ is represented on Figure 15. It can be constructed with Laufer's method (see Appendix 5). The arrow represents the strict transform of a generic linear form $h = \alpha x + \beta y + \gamma z$ on $(X, 0)$. The vertex adjacent to it is the unique $\mathcal{L}$-node and Γ has two nodes which are circled on the figure. The thick-thin decomposition of $(X, 0)$ has one thick piece $(Y_1, 0)$ and one thin piece $(Z_1, 0)$. The subgraph Γ_1' of Γ such that $Y_1 = \pi(N(\Gamma_1'))$ is in black and the subgraph Γ_1 such that $Z_1 = \pi(\mathcal{N}(\Gamma_1))$ is in white.

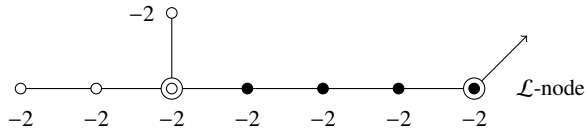


Fig. 15: The thick-thin decomposition of the singularity E_8

Example 3.20. Consider the normal surface singularity $(X, 0) \subset (\mathbb{C}^3, 0)$ with equation $x^2 + zy^2 + z^3 = 0$. This is the standard singularity D_4. Its minimal resolution has exceptional divisor a tree of four $\mathbb{P}^1$'s having self intersections -2 and it factors through the blow-up of the point 0. The dual graph Γ is represented on Figure 16. It has one $\mathcal{L}$-node, which is the central vertex circled on the figure and no other node. Therefore, the thick-thin decomposition of $(X, 0)$ has empty thin part and $(X, 0)$ is metrically conical. The subgraph of Γ corresponding to the thick part is the whole Γ.

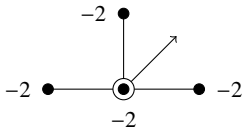


Fig. 16: The thick-thin decomposition of the singularity D_4

Example 3.21. Consider the family of surface singularities in $(X_t, 0) \subset (\mathbb{C}^3, 0)$ with equations $x^5 + z^{15} + y^7 z + txy^6 = 0$ depending on the parameter $t \in \mathbb{C}$. This is a μ-constant family introduced by Briançon and Speder in [BS75]. The thick-thin decomposition changes radically when t becomes 0. Indeed, the minimal resolution graph of every $(X_t, 0)$ is the first graph on Figure 17 while the two other resolution graphs describe the thick-thin decompositions for $t = 0$ and for $t \neq 0$. For $t \neq 0$ it has three thick components and a single thin one. For $t = 0$, it has one component of each type. We refer to [BNP14, Example 15.7] for further details.

Exercise 3.22. Describe the thick-thin decomposition of every ADE surface singularity and show that among them, only A_1 and D_4 are metrically conical (Answer: [BNP14, Example 15.4]). The equations are:

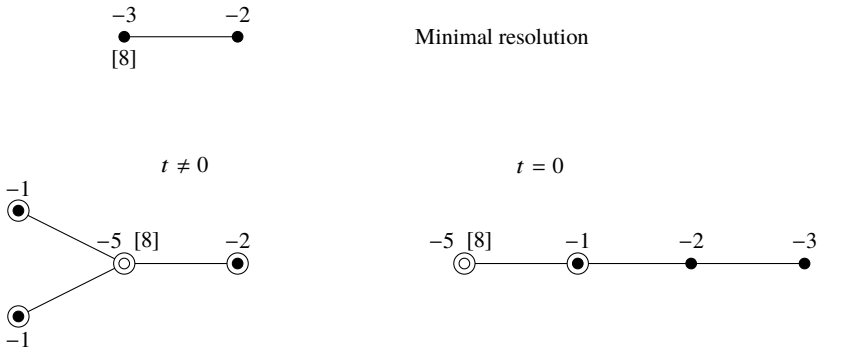


Fig. 17: The two thick-thin decompositions in the Briançon-Speder family $x^5 + z^{15} + y^7 z + txy^6 = 0$

- $A_n : x^2 + y^2 + z^{k+1} = 0, \ k \geq 1$
- $D_n : x^2 + zy^2 + z^{k-1} = 0, \ k \geq 4$
- $E_6 : x^2 + y^3 + z^4 = 0$
- $E_7 : x^2 + y^3 + yz^3 = 0$
- $E_8 : x^2 + y^3 + z^5 = 0$

3.4 Generic projection and inner metric: a key lemma

In this section, we state and prove Lemma 3.29 which is one of the key results which will lead to the complete classification of the inner metric of $(X, 0)$. We give two applications. The first one is the proof of Lemma 3.18. The second describes the inner contact between complex curves on a complex surface.

We first need to introduce the polar curves of generic projections and the Nash modification of $(X, 0)$.

3.4.1 Polar curves and generic projections

Let $(X, 0) \subset (\mathbb{C}^n, 0)$ be a normal surface singularity. We restrict ourselves to those $\mathcal{D}$ in $\mathbf{G}(n-2, \mathbb{C}^n)$ such that the restriction $\ell_{\mathcal{D}}|_{(X,0)} : (X, 0) \to (\mathbb{C}^2, 0)$ is finite. The **polar curve** $\Pi_{\mathcal{D}}$ of $(X, 0)$ for the direction $\mathcal{D}$ is the closure in $(X, 0)$ of the critical locus of the restriction of $\ell_{\mathcal{D}}$ to $X \setminus \{0\}$. The **discriminant curve** $\Delta_{\mathcal{D}} \subset (\mathbb{C}^2, 0)$ is the image $\ell_{\mathcal{D}}(\Pi_{\mathcal{D}})$ of the polar curve $\Pi_{\mathcal{D}}$.

Proposition 3.23 ([Tei82, Lemme-clé V 1.2.2]). *An open dense subset $\Omega \subset \mathbf{G}(n-2, \mathbb{C}^n)$ exists such that:*

1. *The family of curve germs* $(\Pi_{\mathcal{D}})_{\mathcal{D}\in\Omega}$ *is equisingular in terms of strong simultaneous resolution;*
2. *The curves* $\ell_{\mathcal{D}}(\Pi_{\mathcal{D}'})$, $(\mathcal{D},\mathcal{D}')\in\Omega\times\Omega$ *form an equisingular family of reduced plane curves;*
3. *For each* $\mathcal{D}$*, the projection* $\ell_{\mathcal{D}}$ *is generic for its polar curve* $\Pi_{\mathcal{D}}$ *(Definition 2.3).*

Definition 3.24. The projection $\ell_{\mathcal{D}}\colon\mathbb{C}^n\to\mathbb{C}^2$ is **generic** for $(X,0)$ if $\mathcal{D}\in\Omega$.

3.4.2 Nash modification

Definition 3.25. Let $\lambda\colon X\setminus\{0\}\to\mathbf{G}(2,\mathbb{C}^n)$ be the map which sends $x\in X\setminus\{0\}$ to the tangent plane T_xX. The closure X_ν of the graph of λ in $X\times\mathbf{G}(2,\mathbb{C}^n)$ is a reduced analytic surface. By definition, the **Nash modification** of $(X,0)$ is the morphism $\nu\colon X_\nu\to X$ induced by projection on the first factor.

Lemma 3.26 ([Spi90, Part III, Theorem 1.2]). *A morphism* $\pi\colon Y\to X$ *factors through Nash modification if and only if it has no base points for the family of polar curves of generic projections, i.e., there is no point* $p\in\pi^{-1}(0)$ *such that for every* $\mathcal{D}\in\Omega$*, the strict transform of* $\Pi_{\mathcal{D}}$ *by* π *passes through* p*.*

Definition 3.27. Let $(X,0)\subset(\mathbb{C}^n,0)$ be a complex surface germ and let $\nu\colon X_\nu\to X$ be the Nash modification of X. The **Gauss map** $\widetilde{\lambda}\colon X_\nu\to\mathbf{G}(2,\mathbb{C}^n)$ is the restriction to X_ν of the projection of $X\times\mathbf{G}(2,\mathbb{C}^n)$ on the second factor.

Let $\ell\colon\mathbb{C}^n\to\mathbb{C}^2$ be a linear projection such that the restriction $\ell|_X\colon(X,0)\to(\mathbb{C}^2,0)$ is generic. Let Π and Δ be the polar and discriminant curves of $\ell|_X$.

Definition 3.28. The **local bilipschitz constant of** $\ell|_X$ is the map $K\colon X\setminus\{0\}\to\mathbb{R}\cup\{\infty\}$ defined as follows. It is infinite on the polar curve Π and at a point $p\in X\setminus\Pi$ it is the reciprocal of the shortest length among images of unit vectors in T_pX under the projection $\ell\,|_{T_pX}\colon T_pX\to\mathbb{C}^2$.

Let Π^* denote the strict transform of the polar curve Π by the Nash modification ν. Set $B_\epsilon=\{x\in\mathbb{C}^n\colon\|x\|_{\mathbb{C}^n}\leq\epsilon\}$.

Lemma 3.29. *Given any neighbourhood* U *of* $\Pi^*\cap\nu^{-1}(B_\epsilon\cap X)$ *in* $X_\nu\cap\nu^{-1}(B_\epsilon\cap X)$*, the local bilipschitz constant* K *of* $\ell\,|_X$ *is bounded on* $B_\epsilon\cap(X\setminus\nu(U))$*.*

Proof. Let $\kappa\colon\mathbf{G}(2,\mathbb{C}^n)\to\mathbb{R}\cup\{\infty\}$ be the map sending $H\in\mathbf{G}(2,\mathbb{C}^n)$ to the bilipschitz constant of the restriction $\ell|_H\colon H\to\mathbb{C}^2$. The map $\kappa\circ\widetilde{\lambda}$ coincides with $K\circ\nu$ on $X_\nu\setminus\nu^{-1}(0)$ and takes finite values outside Π^*. The map $\kappa\circ\widetilde{\lambda}$ is continuous and therefore bounded on the compact set $\nu^{-1}(B_\epsilon\cap X)\setminus U$.

We will use "small" special versions of U called polar wedges, defined as follows.

Definition 3.30. Let Π_0 be a component of Π and let (u,v) be local coordinates in X_ν centered at $p=\Pi_0^*\cap\nu^{-1}(0)$ such that $v=0$ is the local equation of $\nu^{-1}(0)$. For $\alpha>0$, consider the polydisc $U_{\Pi_0}(\alpha)=\{(u,v)\in\mathbb{C}^2\colon|u|\leq\alpha\}$. For small α, the set $W_{\Pi_0}=\nu(U_{\Pi_0}(\alpha))$ is called a **polar wedge** around Π_0 and the union $W=\bigcup_{\Pi_0\subset\Pi}W_{\Pi_0}$ a **polar wedge** around Π.

3.4.3 Application 1

Proof (of Lemma 3.18). We want to prove that for every $\mathcal{L}$-node ν, the germ $\pi(\mathscr{N}(\nu))$ is metrically conical.

Consider a polar wedge W around Π. A direct consequence of Lemma 3.29 is that the restriction of ℓ to $X \setminus W$ is a local bilipschitz homeomorphism for the inner metric. Therefore, for any metrically conical germ C in $(\mathbb{C}^2, 0)$, the intersection of the lifting $\ell^{-1}(C)$ with $\overline{X \setminus W}$ will be a metrically conical germ.

For each $j = 1, \ldots, s$, let $L_j \subset \mathbb{C}^n$ be the complex tangent line of the thin germ $(Z_j, 0)$ and let $L'_j \subset \mathbb{C}^2$ be image of L_j by the generic linear form $\ell \colon \mathbb{C}^n \to \mathbb{C}^2$. Assume L'_j has equation $y = a_j x$. For a real number $\alpha > 0$, we consider the conical subset $V_\alpha \subset \mathbb{C}^2$ defined as the union of the complex lines $y = \eta x$ such that $|\eta - a_j| \geq \alpha$, so V_α is the closure of a set obtained by removing conical neighbourhoods of the lines L'_j. Applying the above result, we obtain that for all $\alpha > 0$, the intersection of the lifting $\ell^{-1}(V_\alpha)$ with $\overline{X \setminus W}$ gives a metrically conical germ at 0. Since there exist two real numbers α_1, α_2 with $0 < \alpha_1 < \alpha_2$ such that inside a small ball B_ϵ, we have $\ell^{-1}(V_{\alpha_1}) \subset \pi(\mathscr{N}(\nu)) \subset \ell^{-1}(V_{\alpha_2})$, then the germ $\pi(\mathscr{N}(\nu)) \cap (\overline{X \setminus W})$ at 0 is also metrically conical.

If the strict transform of Π by π does not intersect the $\mathcal{L}$-curve E_ν, then the intersection $\pi(\mathscr{N}(\nu)) \cap (\overline{X \setminus W})$ is the whole $\pi(\mathscr{N}(\nu))$. Therefore $\pi(\mathscr{N}(\nu))$ is metrically conical.

If the strict transform of Π by π intersects the $\mathcal{L}$-curve E_ν, then we have to use a second generic projection $\ell' \colon (X, 0) \to (\mathbb{C}^2, 0)$ such that the strict transform of the polar curve Π' of ℓ' by π does not intersect U, and we prove that $\overline{\pi(\mathscr{N}(\nu)) \cap W}$ is metrically conical using the above argument. Therefore $\pi(\mathscr{N}(\nu))$ is metrically conical as the union of two metrically conical sets.

3.4.4 Application 2.

Let $(X, 0)$ be a normal complex surface singularity.

Definition 3.31. Let $S_\epsilon = \{x \in \mathbb{C}^n \colon \|x\|_{\mathbb{C}^n} = \epsilon\}$. Let $(\gamma, 0)$ and $(\gamma', 0)$ be two distinct irreducible germs of complex curves inside $(X, 0)$. Let $q_{inn} = q_{inn}(\gamma, \gamma')$ be the rational number ≥ 1 defined by

$$d_i(\gamma \cap S_\epsilon, \gamma' \cap S_\epsilon) = \Theta(\epsilon^{q_{inn}}),$$

where d_i means inner distance in $(X, 0)$ as before.

We call $q_{inn}(\gamma, \gamma')$ the *the inner contact exponent* or *inner contact order* between γ and γ'.

The proof of the existence and rationality of the inner contact q_{inn} needs deep arguments of [KO97]. We refer to this paper for details.

Remark 3.32. One can also define the outer contact exponent q_{out} between two curves by using the outer metric instead of the inner one. In that case, the existence and rationality of q_{out} come easily from the fact that the outer distance d_o is a semialgebraic function. (While the inner distance d_i is not semi-algebraic.)

Definition 3.33. Let $\pi\colon Z \to X$ be a resolution of X and let E be an irreducible component of the exceptional divisor $\pi^{-1}(0)$. A *curvette* of E is a smooth curve $\delta \subset Z$ which is transversal to E at a smooth point of the exceptional divisor $\pi^{-1}(0)$.

Lemma 3.34. *[NPP19a, Lemma 15.1] Let $\pi\colon Z \to X$ be a resolution of $(X,0)$ and let E be an irreducible component of the exceptional divisor $\pi^{-1}(0)$. Let $(\gamma,0)$ and $(\gamma',0)$ be the π-images of two curvettes of E meeting E at two distinct points. Then $q_{inn}(\gamma,\gamma')$ is independent of the choice of γ and γ'.*

Definition 3.35. We set $q_E = q_{inn}(\gamma,\gamma')$ and we call q_E the *inner rate* of E.

Remark 3.36. When $X = \mathbb{C}^2$, inner and outer metrics coincide and the result is well known and comes from classical plane curve theory: in that case, $q_{inn}(\gamma,\gamma')$ is the coincidence exponent between Puiseux expansions of the curves γ and γ' (see for example [GBT99, page 401]). The inner rate at each vertex of a sequence of blow-ups can be computed by using the classical dictionary between characteristic exponents of an irreducible curve and its resolution graph. We refer to [EN85, page 148] or [Wal04, Section 8.3] for details. As a consequence of this, the inner rates along any path from the root vertex to a leaf of T form a strictly increasing sequence.

Example 3.37. The dual tree T_0 of the minimal resolution $\sigma_0\colon Y_0 \to \mathbb{C}^2$ of the curve γ with Puiseux expansion $y = z^{5/3}$ is obtained (Figure 18) by computing the continued fraction development

$$\frac{5}{3} = 1 + \frac{1}{1+\frac{1}{2}} =: [1,1,2]^+.$$

Since $1+1+2 = 4$, σ_0 consists of four successive blow-ups of points starting with the blow-up of the origin of $\mathbb{C}^2$ which correspond to the four vertices of T_0. The irreducible curves $E_1,\dots,E_4$ are labelled in their order of appearance and the vertices of T_0 are also weighted by their self-intersections E_i^2.

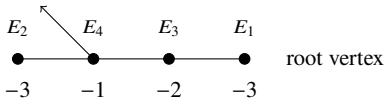


Fig. 18: The resolution tree T_0 of the curve $x^5 + z^{15} + y^7 z + txy^6 = 0$

The inner rates are computed by using the approximation numbers associated with the sequence $[1,1,2]^+$: $q_{v_1} = [1]^+ = 1$, $q_{v_2} = [1,1]^+ = 1+\frac{1}{1} = 2$, $q_{v_3} = [1,1,1]^+ = \frac{3}{2}$ and $q_{v_3} = [1,1,2]^+ = \frac{5}{3}$

This gives the tree T_0 of Figure 19 where each vertex is weighted by the self intersection of the corresponding exceptional curve E_i and with the inner rate q_{E_i} (in bold).

Let us blow up every intersection point between irreducible components of the total transform $\sigma_0^{-1}(\gamma)$. The resulting tree T is that used to compute the dual resolution graph of $E_8\colon x^2+y^3-z^5=0$ by Laufer's method (Appendix 5). Again, the inner rates are in bold. Their computation is left to the reader as an exercise.

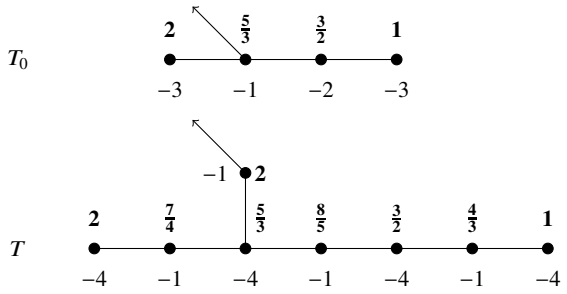


Fig. 19: The inner rates in resolutions of the curve $y=x^{5/3}$

Proof (of Lemma 3.34). Consider a generic projection $\ell\colon (X,0)\to(\mathbb{C}^2,0)$ which is also generic for the curve germ $(\gamma\cup\gamma',0)$ (Definition 2.3). Then consider the minimal sequence of blow-ups $\sigma\colon Y\to\mathbb{C}^2$ such that the strict transforms $\ell(\gamma)^*$ and $\ell(\gamma')^*$ by σ do not intersect. Then $\ell(\gamma)^*$ and $\ell(\gamma')^*$ are two curvettes of the last exceptional curve C created by σ and we then have $q_{inn}(\ell(\gamma),\ell(\gamma'))=q_C$. Moreover, an easy argument using Hirzebruch-Jung resolution of surfaces (see [PP11] for an introduction to this resolution method) shows that σ does not depend on the choice of the curvettes γ^* and γ'^* of E. Now, since ℓ is generic for the curve $\gamma\cup\gamma'$, the strict transform of the polar curve Π of ℓ by π does not intersect the strict transform of $\gamma\cup\gamma'$, and then, $\gamma^*\cup\gamma'^*$ is outside any sufficiently small polar wedge of ℓ around Π. Therefore, by Lemma 3.29, we obtain $q_{inn}(\gamma,\gamma')=q_{inn}(\ell(\gamma),\ell(\gamma'))=q_C$

Example 3.38. The proof of Lemma 3.34 shows that the inner rates q_E can be computed by using inner rates in $\mathbb{C}^2$ through a generic projection $\ell\colon (X,0)\to(\mathbb{C}^2,0)$. Applying this, Figure 20 shows the inner rate at each vertex of the minimal resolution graph of the surface singularity $E_8\colon x^2+y^3+z^5=0$. They are obtained by lifting the inner rates of the graph T of Example 3.37.

3.5 *Fast loops in the thin pieces*

Consider a normal surface germ $(X,0)\subset(\mathbb{C}^n,0)$. We choose coordinates $(z_1\ldots,z_n)$ in $\mathbb{C}^n$ so that z_1 and z_2 are generic linear forms and $\ell:=(z_1,z_2)\colon X\to\mathbb{C}^2$ is a

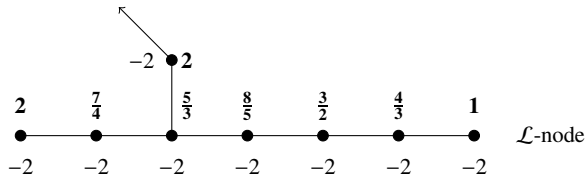


Fig. 20: The inner rates for the singularity E_8

generic linear projection. The family of Milnor balls we use in the sequel consists of standard "Milnor tubes" associated with the Milnor-Lê fibration for the map $\zeta := z_1|_X : X \to \mathbb{C}$ Namely, for some sufficiently small ϵ_0 and some $R > 0$ we define for $\epsilon \leq \epsilon_0$:

$$B_\epsilon := \{(z_1, \ldots, z_n) \in \mathbb{C}^n : |z_1| \leq \epsilon, \|(z_1, \ldots, z_n)\| \leq R\epsilon\} \quad \text{and} \quad S_\epsilon = \partial B_\epsilon.$$

By [BNP14, Proposition 4.1], on can choose ϵ_0 and R so that for $\epsilon \leq \epsilon_0$:

1. $\zeta^{-1}(t)$ intersects the round sphere

$$S^{2n-1}_{R\epsilon} = \{(z_1, \ldots, z_n) \in \mathbb{C}^n : \|(z_1, \ldots, z_n)\| = R\epsilon\}$$

transversely for $|t| \leq \epsilon$;
2. the polar curve of the projection $\ell = (z_1, z_2)$ meets S_ϵ in the part $|z_1| = \epsilon$.

If $(A, 0)$ is a semialgebraic germ, we denote by $A^{(\epsilon)} = S_\epsilon \cap X$ its link with respect to the Milnor ball B_ϵ.

Theorem 3.39. *[BNP14, Theorem 1.7] Consider the minimal thick-thin decomposition*

$$(X, 0) = \bigcup_{i=1}^{r} (Y_i, 0) \cup \bigcup_{j=1}^{s} (Z_j, 0)$$

of $(X, 0)$. *For* $0 < \epsilon \leq \epsilon_0$ *and for each* $j = 1, \ldots, s$, *let* $\zeta_j^{(\epsilon)} : Z_j^{(\epsilon)} \to S^1$ *be the restriction to* $Z_j^{(\epsilon)}$ *of the generic linear form* $h = z_1$. *Then there exists* $q_j > 1$ *such that the fibers* $\zeta_j^{-1}(t)$ *have diameter* $\Theta(\epsilon^{q_j})$.

Proof (Sketch of proof of Theorem 3.39). The proof of Theorem 3.39 is based on two keypoints: Lemma 3.29, which implies that ℓ is an inner Lipschitz homeomorphism outside a polar wedge W, and the so called Polar Wedge Lemma [BNP14, Proposition 3.4] which describes the geometry of a polar wedge. The idea is to use a generic linear projection $\ell = (z_1, z_2) : (X, 0) \to (\mathbb{C}^2, 0)$ and to describe $(Z_j, 0)$ as a component of the lifting by ℓ of some semi-algebraic germ $(V_j, 0)$ in $\mathbb{C}^2$ which has the properties described in the Theorem, i.e., for small $\epsilon > 0$, $V_j^{(\epsilon)}$ fibers over S^1 with fibers having diameter $\Theta(\epsilon^{q_j})$ for some $q_j > 1$.

Consider a sequence $\sigma : Y \to \mathbb{C}^2$ of blow-ups of points which resolves the base points of the family of projected polar curves $\ell(\Pi_{\mathcal{D}})_{\mathcal{D} \in \Omega}$ and let T be its dual tree.

Notice that the strict transforms of the curves $\ell(\Pi_{\mathcal{D}})$, $\mathcal{D} \in \Omega$ form an equisingular family of complex curves, but that these curves are not necessarily smooth, i.e., σ is not, in general, a resolution of $\ell(\Pi_{\mathcal{D}})$.

Denote by v_1 the root vertex of T, i.e., the vertex corresponding to the exceptional curve created by the first blow-up and by T_0 the subtree of T consisting of v_1 union any adjacent string or bamboo. Then Z_j is a component of $\ell^{-1}(V_j)$ where $V_j = \sigma(\mathcal{N}(T_j))$ and where T_j is a component of $T \setminus T_0$. Let v_j be the vertex of T_j adjacent to T_0. By classical curve theory, V_j is a set of the form $V_j = \{z_2 = \lambda z_1^{q_j}, a \leq |\lambda| \leq b\}$, where q_j is the inner rate of the exceptional curve represented by the vertex v_j. In particular, the 3-manifold $V_j^{(\epsilon)} = V_j \cap \{|z_1| = \epsilon\}$ is fibered over the circle S^1_ϵ by the projection $z_1 : V_j^{(\epsilon)} \to S^1_\epsilon$ and the fibers have diameter $\Theta(\epsilon^{q_j})$.

Let W be a polar wedge around Π. By Lemma 3.29, we know that ℓ is a locally inner bilipschitz homeomorphism outside W. Therefore, the fibers of the restriction $\zeta_j^{(\epsilon)} : Z_j^{(\epsilon)} \setminus W^{(\epsilon)} \to S^1$ have diameter $\Theta(\epsilon^{q_j})$. Moreover the Polar Wedge Lemma [BNP14, Proposition 3.4] guarantees that the fibers of the restriction of $\zeta_j^{(\epsilon)}$ to the link of a component of a polar wedge inside $(Z_j, 0)$ have diameter at most $\Theta(\epsilon^{q_j})$.

In [BNP14, Section 7], it is proved that each $Z_j^{(\epsilon)}$ contains loops which are essential in $X^{(\epsilon)}$. As a consequence of Theorem 3.39, we obtain the existence of families of fast loops γ_ϵ inside each $Z_j^{(\epsilon)}$.

4 Geometric decompositions of a surface singularity

In this part, we explain how to break the thin pieces of the thick-thin decomposition into standard pieces which are still invariant by bilipschitz change of the inner metric. The resulting decomposition of $(X, 0)$ is what we call the inner geometric decomposition of $(X, 0)$. Then, we will define the outer geometric decomposition of $(X, 0)$, which is a refinement of the inner one, and which is invariant by bilipschitz change of the outer metric.

The inner and outer geometric decompositions will lead to several key results:

1. The complete classification of the inner Lipschitz geometry of a normal surface germ (Theorem 4.30);
2. A refined geometric decomposition which is an invariant of the outer Lipschitz geometry (Theorem 4.36);
3. A list of analytic invariants of the surface which are in fact invariants of the outer Lipschitz geometry (Theorem 4.38);

4.1 The standard pieces

In this section, we introduce the standard pieces of our geometric decompositions. We refer to [BNP14, Sections 11 and 13] for more details.

The pieces are topologically conical, but usually with metrics that make them shrink non-linearly towards the cone point. We will consider these pieces as germs at their cone-points, but for the moment, to simplify notation, we suppress this.

4.1.1 The B-pieces

Let us start with a prototype which already appeared earlier in these notes (Example 3.7). Choose $q > 1$ in $\mathbb{Q}$ and $0 < a < b$ in $\mathbb{R}$. Let $Z \in \mathbb{C}^2$ be defined as the semi-algebraic set

$$Z := \{(x, y) \subset \mathbb{C}^2 : y = \lambda x^q, a \leq |\lambda| \leq b\}.$$

Then for all $\epsilon > 0$, the intersection $Z^{(\epsilon)} = Z \cap \{|x| = \epsilon\}$ is a 3-manifold (namely a thickened torus) and the restriction of the function x to $Z^{(\epsilon)}$ defines a locally trivial fibration $x\colon Z^{(\epsilon)} \to S^1_\epsilon$ whose fibers are annuli with diameter $\Theta(\epsilon^q)$.

Definition 4.1 ($B(q)$-pieces). Let F be a compact oriented 2-manifold, $\phi\colon F \to F$ an orientation preserving diffeomorphism, and M_ϕ the mapping torus of ϕ, defined as:

$$M_\phi := ([0, 2\pi] \times F)/((2\pi, x) \sim (0, \phi(x))) .$$

Given a rational number $q > 1$, we will define a metric space $B(F, \phi, q)$ which is topologically the cone on the mapping torus M_ϕ.

For each $0 \leq \theta \leq 2\pi$ choose a Riemannian metric g_θ on F, varying smoothly with θ, such that for some small $\delta > 0$:

$$g_\theta = \begin{cases} g_0 & \text{for } \theta \in [0, \delta], \\ \phi^* g_0 & \text{for } \theta \in [2\pi - \delta, 2\pi] . \end{cases}$$

Then for any $r \in (0, 1]$ the metric $r^2 d\theta^2 + r^{2q} g_\theta$ on $[0, 2\pi] \times F$ induces a smooth metric on M_ϕ. Thus

$$dr^2 + r^2 d\theta^2 + r^{2q} g_\theta$$

defines a smooth metric on $(0, 1] \times M_\phi$. The metric completion of $(0, 1] \times M_\phi$ adds a single point at $r = 0$. Denote this completion by $B(F, \phi, q)$. We call a metric space which is bilipschitz homeomorphic to $B(F, \phi, q)$ a $B(q)$**-piece** or simply a B**-piece**.

A $B(q)$-piece such that F is a disc is called a $D(q)$**-piece** or simply a D**-piece**.

A $B(q)$-piece such that F is an annulus $S^1 \times [0, 1]$ is called an $A(q, q)$-piece.

Example 4.2. The following is based on classical theory of plane curve singularities and is a generalization of the prototype given before Definition 4.1. Let $\sigma\colon Y \to \mathbb{C}^2$ be a sequence of blow-ups of points starting with the blow-up of the origin and let E_i

be a component of $\sigma^{-1}(0)$ which is not the component created by the first blow-up. Then the inner rate q_{E_i} is strictly greater than 1, $B_i = \sigma(\mathscr{N}(E_i))$ is a $B(q_{E_i})$-piece fibered by the restriction of a generic linear form and the fiber consists of a disc minus a finite union of open discs inside it.

This is based on the fact that in suitable coordinates (x, y), one may construct such a piece B_i as a union of curves $\gamma_\lambda \colon y = \sum_{k=1}^{m} a_k x^{p_k} + \lambda x^{q_{E_i}}$, where $p_1 < \ldots < p_m < q_{E_i}$. Here $y = \sum_{k=1}^{m} a_k x^{p_k}$ is the common part of their Puiseux series and the coefficient $\lambda \in \mathbb{C}^*$ varies in a compact disc minus a finite union of open discs inside it.

Notice that if E_i intersects exactly one other exceptional curve E_j, then one gets a $D(q_{E_i})$-piece. If E_i intersects exactly two other curves E_j and E_k, one gets an $A(q_{E_i}, q_{E_i})$-piece.

4.1.2 The A-pieces

Again, we start with a prototype. Choose $1 \leq q < q'$ in $\mathbb{Q}$ and $0 < a$ in $\mathbb{R}$ and let $Z \subset \mathbb{C}^2$ be defined as the semi-algebraic set

$$Z := \{(x, y) \subset \mathbb{C}^2 : y = \lambda x^s, |\lambda| = a, q \leq s \leq q'\}\,.$$

Then for all $\epsilon > 0$, the intersection $Z^{(\epsilon)} = Z \cap \{|x| = \epsilon\}$ is a thickened torus whose restriction of the function x to $Z^{(\epsilon)}$ defines a locally trivial fibration $x \colon Z^{(\epsilon)} \to S^1_\epsilon$ whose fibers are flat annuli with outer boundary of length $\Theta(\epsilon^q)$ and inner boundary of length $\Theta(\epsilon^{q'})$.

Definition 4.3 ($A(q, q')$-pieces). Let q, q' be rational numbers such that $1 \leq q \leq q'$. Let A be the Euclidean annulus $\{(\rho, \psi) : 1 \leq \rho \leq 2, 0 \leq \psi \leq 2\pi\}$ in polar coordinates and for $0 < r \leq 1$ let $g^{(r)}_{q,q'}$ be the metric on A:

$$g^{(r)}_{q,q'} := (r^q - r^{q'})^2 d\rho^2 + ((\rho - 1)r^q + (2 - \rho)r^{q'})^2 d\psi^2\,.$$

Endowed with this metric, A is isometric to the Euclidean annulus with inner and outer radii $r^{q'}$ and r^q. The metric completion of $(0, 1] \times \S^1 \times A$ with the metric

$$dr^2 + r^2 d\theta^2 + g^{(r)}_{q,q'}$$

compactifies it by adding a single point at $r = 0$. We call a metric space which is bilipschitz homeomorphic to this completion an $A(q, q')$**-piece** or simply an A**-piece**.

Notice that when $q = q'$, this definition of $A(q, q)$ coincides with that introduced in Definition 4.1.

Example 4.4. Let $\sigma \colon Y \to \mathbb{C}^2$ be as in Example 4.2 and let T be its dual tree. As already mentioned in Remark 3.36, the inner rates along any path from the root vertex to a leaf of T form a strictly increasing sequence. In particular, any edge e in T joins two vertices v and v', with inner rates respectively q and q' with $1 \leq q < q'$.

Moreover, the semialgebraic set $Z = \sigma(N(v) \cap N(v'))$ is an $A(q, q')$-piece fibered by the restriction of a generic linear form and is bounded by the $B(q)$- and $B(q')$-pieces $\sigma(\mathscr{N}(v))$ and $\sigma(\mathscr{N}(v'))$.

More generally, let $S \subset T$ be a string in T which does not contain the root vertex of T. let $1 < q < q'$ be the two inner rates associated with the two vertices adjacent to S. Then $Z = \sigma(N(S))$ is an $A(q, q')$-piece fibered by the restriction of a generic linear form.

Definition 4.5 (Rate). The rational number q is called the **rate** of $B(q)$ or $D(q)$. The rational numbers q and q' are the two **rates** of $A(q, q')$.

4.1.3 **Conical pieces** (or $B(1)$-pieces)

Definition 4.6 (Conical pieces). Given a compact smooth 3-manifold M, choose a Riemannian metric g on M and consider the metric $dr^2 + r^2 g$ on $(0, 1] \times M$. The completion of this adds a point at $r = 0$, giving a **metric cone on** M. We call a metric space which is bilipschitz homeomorphic to a metric cone a **conical piece** or a $B(1)$**-piece** (they were called CM-pieces in [BNP14]).

Example 4.7. Let $\sigma : Y \to X$ and T be as in Example 4.2 and let v_1 be the root vertex of T. Then $\sigma(\mathscr{N}(v_1))$ is a conical piece.

4.2 Geometric decompositions of $\mathbb{C}^2$

A geometric decomposition of a semi-algebraic germ $(Y, 0)$ consists of a decomposition of $(Y, 0)$ as a union of A, B and conical pieces glued along their boundary components in such a way that the fibrations of B and A pieces coincide on the gluing.

Examples 4.2, 4.4 and 4.7 show that any sequence $\sigma : Y \to \mathbb{C}^2$ of blow-ups of points starting with the blow-up of the origin defines a geometric decomposition of $(\mathbb{C}^2, 0)$ whose B-pieces are in bijection with the exceptional curves E_i in $\sigma^{-1}(0)$ and the intermediate $A(q, q')$-pieces, $q < q'$ with the intersection points $E_i \cap E_j$.

Definition 4.8. We call this geometric decomposition of $(\mathbb{C}^2, 0)$ the geometric decomposition associated with σ.

Example 4.9. Consider the minimal resolution σ of the curve germ γ with Puiseux expansion $y = x^{3/2} + x^{7/4}$. Its resolution tree T, with exceptional curves E_i labelled in order of occurence in the sequence of blow-ups, is pictured on Figure 21. Each vertex is also weighted by the corresponding self-intersection E_i^2 and by the inner rate q_{E_i} in bold. The inner rates $q_{E_1} = 1, q_{E_2} = 2$ and $q_{E_3} = \frac{3}{2}$ are computed as in example 3.37 using the first characteristic exponent $\frac{3}{2} = [1, 2]^+$. The two last inner rates are computed using the characteristic Puiseux exponents $\frac{3}{2}$ and $\frac{7}{4}$ as follows.

Set $\frac{p_1}{q_1} = \frac{3}{2}$ and $\frac{p_2}{q_2} = \frac{7}{4}$ and write $\frac{p_2}{q_2} = \frac{p_1}{q_1} + \frac{1}{q_1}\frac{p_2'}{q_2'}$. Then the two last inner rates are computed by using the continued fraction development $\frac{p_2'}{q_2'} = [a_1, \ldots, a_r]^+$. In our case, we have $\frac{7}{4} = \frac{3}{2} + \frac{1}{2}.\frac{1}{2}$, so $\frac{p_2'}{q_2'} = \frac{1}{2} = [0, 2]^+$. This gives $q_{E_4} = \frac{3}{2} + \frac{1}{1} = \frac{5}{2}$ and $q_{E_5} = \frac{3}{2} + \frac{1}{2} = \frac{7}{4}$. (Again, we refer to [EN85] or [Wal04] for details on these computations).

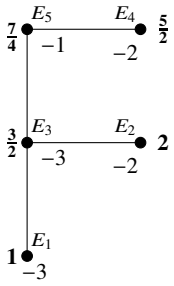


Fig. 21: Geometric decomposition of $(\mathbb{C}^2, 0)$ associated with the resolution of the curve $y = x^{3/2} + x^{7/4}$

The underlying geometric decomposition of $(\mathbb{C}^2, 0)$ consists of:

- Five B-pieces $\sigma(\mathcal{N}(E_i)), i = 1, \ldots, 5$ in bijection with the vertices of T having rates respectively $1, 2, \frac{3}{2}, \frac{5}{2}, \frac{7}{4}$. Notice that the B-pieces corresponding to E_2 and E_4 are respectively a $D(2)$- and a $D(\frac{5}{2})$-piece since the corresponding vertices have valence one.
- Four A-pieces in bijection with the edges of T: $\sigma(N(E_1) \cap N(E_3)), \sigma(N(E_3) \cap N(E_2)), \sigma(N(E_3) \cap N(E_5))$ and $\sigma(N(E_5) \cap N(E_4))$ which are respectively an $A(1, \frac{3}{2})$-piece, an $A(\frac{3}{2}, 2)$-piece, an $A(\frac{3}{2}, \frac{7}{4})$-piece and an $A(\frac{7}{4}, \frac{5}{2})$-piece.

Example 4.10. The trees T_0 and T in Example 3.37 describe two different geometric decompositions of $(\mathbb{C}^2, 0)$ associated with two resolutions of the curve $y = x^{5/3}$.

The following lemma shows that one can simplify a geometric decomposition by amalgamating pieces. In this lemma $\cong$ means bilipschitz equivalence and $\cup$ represents gluing along appropriate boundary components by an isometry. D^2 means the standard 2-disc.

Lemma 4.11. *[Amalgamation Lemma]*

1. $B(D^2, \phi, q) \cong B(D^2, id, q)$; $B(S^1 \times I, \phi, q) \cong B(S^1 \times I, id, q)$.
2. $A(q, q') \cup A(q', q'') \cong A(q, q'')$.
3. *If F is the result of gluing a surface F' to a disk D^2 along boundary components then* $B(F', \phi|_{F'}, q) \cup B(D^2, \phi|_{D^2}, q) \cong B(F, \phi, q)$.
4. $A(q, q') \cup B(D^2, id, q') \cong B(D^2, id, q)$.

5. *Each* $B(D^2, id, 1)$, $B(S^1 \times I, id, 1)$ *or* $B(F, \phi, 1)$ *piece is a conical piece and a union of conical pieces glued along boundary components is a conical piece.* □

Example 4.12. Consider again the geometric decomposition of $(\mathbb{C}^2, 0)$ introduced in Example 4.9. We can amalgamate the $D(2)$-piece union the $A(\frac{3}{2}, 2)$-piece to the neighbour $B(\frac{3}{2})$-piece. We can also amalgamate the $D(\frac{5}{2})$-piece union the adjacent $A(\frac{7}{4}, \frac{5}{2})$-piece to the neighbour $B(\frac{7}{4})$-piece. This produces a geometric decomposition of $(\mathbb{C}^2, 0)$ represented by the tree of Figure 22, where we write inner rates only at the central vertices of B-pieces and not at the amalgamated pieces. This decomposition has five pieces: a conical $B(1)$ (black vertex), a $B(\frac{3}{2})$-piece (red vertices), a $B(\frac{7}{4})$-piece (blue vertices) and intermediate $A(1, \frac{3}{2})$- and $A(\frac{7}{4}, \frac{5}{2})$-pieces.

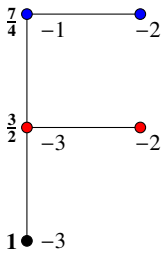


Fig. 22: Amalgamated geometric decomposition

Remark 4.13. Notice that the new $B(\frac{7}{4})$-piece is now a D-piece. Then we could continue the amalgamation process by amalgamating iteratively all D-pieces. Of course, in the case of a geometric decomposition of $(\mathbb{C}^2, 0)$, an iterative amalgamation of the pieces always produces eventually a unique conical piece which is the whole $(\mathbb{C}^2, 0)$.

Example 4.14. In the tree T_0 of Example 4.10, the amalgamation of the $D(2)$-piece union the $A(\frac{5}{3}, 2)$-piece to the neighbour $B(\frac{5}{3})$-piece forms a bigger $B(\frac{5}{3})$-piece. The amalgamation of the $A(\frac{3}{2}, \frac{3}{2})$-piece with the two neighbour $A(1, \frac{3}{2})$- and $A(\frac{3}{2}, \frac{5}{3})$-pieces creates an intermediate $A(1, \frac{5}{3})$-piece between the $B(1)$- and the $B(\frac{5}{3})$-pieces. This creates a new geometric decomposition of $(\mathbb{C}^2, 0)$ with two B-pieces and one A-piece represented on Figure 23. The red vertices correspond to the $B(\frac{5}{3})$-piece and the white one to the A-piece.

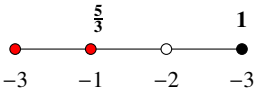


Fig. 23: Amalgamated geometric decomposition for the curve $y = x^{5/3}$

4.3 The Polar Wedge Lemma

Let $(X,0) \subset (\mathbb{C}^2,0)$ be a normal surface singularity. Consider a linear projection $\mathbb{C}^n \to \mathbb{C}^2$ which is generic for $(X,0)$ (e.g. [NPP19a, Definition 2.4]) and denote again by $\ell\colon (X,0) \to (\mathbb{C}^2,0)$ its restriction to $(X,0)$. Let Π be the polar curve of ℓ and let $\Delta = \ell(\Pi)$ be its discriminant curve.

Proposition 4.15 (Polar Wedge Lemma). *[BNP14, 3.4] Consider the resolution $\sigma\colon Y \to \mathbb{C}^2$ which resolves the base points of the family of projections of generic polar curves $(\ell(\Pi_{\mathcal{D}}))_{\mathcal{D}\in\Omega}$. Let Π_0 be an irreducible component of Π and let $\Delta_0 = \ell(\Pi_0)$. Let C be the irreducible component of $\sigma^{-1}(0)$ which intersects the strict transform of Δ_0^* by σ.*

Let W_{Π_0} be a polar wedge around Π_0 as introduced in Definition 3.30. Then W_{Π_0} is a $D(q_C)$-piece, and when $q_C > 1$, W_{Π_0} is fibered by its intersections with the real surfaces $\{h = t\} \cap X$, where $h\colon \mathbb{C}^n \to \mathbb{C}$ is a generic linear form.

4.4 The geometric decomposition and the complete Lipschitz classification for the inner metric

Let $(X,0)$ be a surface germ, let $\ell\colon (X,0) \to (\mathbb{C}^2,0)$ be a generic linear projection with polar curve Π and let W be a polar wedge around Π. Let $\sigma\colon Y \to \mathbb{C}^2$ be the minimal sequence of blow-ups which resolves the base points of the family of projected polar curves $(\ell(\Pi_{\mathcal{D}}))_{\mathcal{D}\in\Omega}$ and consider the geometric decomposition of $(\mathbb{C}^2,0)$ associated with σ (Definition 4.8).

Definition 4.16. Let T be the resolution tree of σ. We call Δ-*curve* any component of $\sigma^{-1}(0)$ which intersects the strict transform of the discriminant curve Δ of ℓ, and we call Δ-*node* of T any vertex representing a Δ-curve.

We call *node* of T any vertex which is either the root-vertex or a Δ-node or a vertex with valence ≥ 3.

Using Lemma 4.11, we amalgamate iteratively all the D-pieces of the geometric decomposition of $(\mathbb{C}^2,0)$ associated with σ with the rule that we never amalgamate a piece containing a component of the discriminant curve Δ of ℓ. We then obtain a geometric decomposition of $(\mathbb{C}^2,0)$ whose pieces are in bijection with the nodes of T.

Definition 4.17. We call this decomposition *the geometric decomposition of* $(\mathbb{C}^2,0)$ *associated with the projection* $\ell\colon (X,0) \to (\mathbb{C}^2,0)$.

Example 4.18. Consider again the germ $(X,0)$ of the surface E_8 with equation $x^2 + y^3 + z^5 = 0$ and the projection $\ell\colon (x,y,z) \to (y,z)$. In order to compute the geometric decomposition of $(\mathbb{C}^2,0)$ associated with ℓ, we need to compute a resolution graph of $\sigma\colon Y \to \mathbb{C}^2$ as defined above with its inner rates. We will first compute the minimal resolution of $(X,0)$ which factors through Nash modification.

We first consider the graph Γ of the minimal resolution π of E_8 as computed in the Appendix of the present notes. We add to Γ decorations by arrows corresponding to the strict transforms of the coordinate functions x, y and $z\colon (X,0) \to (\mathbb{C},0)$ and we denote the exceptional curves by $E_i, i = 1,\dots,8$ (the order is random). All the self-intersections of the exceptional curves equal -2 so we do not write them on the graph. We obtain the graph of Figure 24.

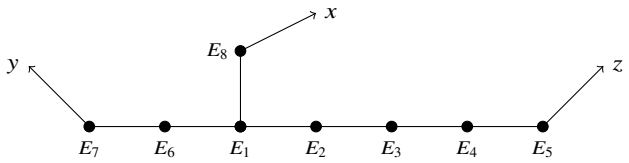


Fig. 24: Resolution of the coordinates functions on the E_8 singularity

Let $h\colon (X,0) \to (\mathbb{C},0)$ be an analytic function, and let $(h\circ\pi) = \sum_{j=1}^{8} m_j E_j + h^*$ be its total transform by π, so m_j denotes the multiplicity of h along E_j and h^* its strict transform by π. Then, for all $j = 1,\dots,8$, we have $(h\circ\pi).E_j = 0$ ([Lau71, Theorem 2.6]). Using this, we compute the total transforms by π of the coordinate functions x, y and z:

$$\begin{aligned}(x\circ\pi) &= 15E_1 + 12E_2 + 9E_3 + 6E_4 + 3E_5 + 10E_6 + 5E_7 + 8E_8 + x^*\\ (y\circ\pi) &= 10E_1 + 8E_2 + 6E_3 + 4E_4 + 2E_5 + 7E_6 + 4E_7 + 5E_8 + y^*\\ (z\circ\pi) &= 6E_1 + 5E_2 + 4E_3 + 3E_4 + 2E_5 + 4E_6 + 2E_7 + 3E_8 + z^*\end{aligned}$$

Set $f(x,y,z) = x^2 + y^3 + z^5$. The polar curve Π of a generic linear projection $\ell\colon (X,0) \to (\mathbb{C}^2,0)$ has equation $g = 0$ where g is a generic linear combination of the partial derivatives $f_x = 2x$, $f_y = 3y^2$ and $f_z = 5z^4$. The multiplicities of g are given by the minimum of the compact part of the three divisors

$$\begin{aligned}(f_x\circ\pi) &= 15E_1 + 12E_2 + 9E_3 + 6E_4 + 3E_5 + 10E_6 + 5E_7 + 8E_8 + f_x^*\\ (f_y\circ\pi) &= 20E_1 + 16E_2 + 12E_3 + 8E_4 + 4E_5 + 14E_6 + 8E_7 + 10E_8 + f_y^*\\ (f_z\circ\pi) &= 24E_1 + 20E_2 + 16E_3 + 12E_4 + 8E_5 + 16E_6 + 8E_7 + 12E_8 + f_z^*\end{aligned}$$

We then obtain that the total transform of g is equal to:

$$(g\circ\pi) = 15E_1 + 12E_2 + 9E_3 + 6E_4 + 3E_5 + 10E_6 + 5E_7 + 8E_8 + \Pi^*\,.$$

In particular, Π is resolved by π and its strict transform Π^* has just one component, which intersects E_8.

Exercise 4.19. 1. Prove that since the multiplicities $m_8(f_x) = 8$, $m_8(f_y) = 10$ and $m_8(z) = 12$ along E_8 are distinct, the family of polar curves, i.e., the linear system generated by f_x, f_y and f_z, has a base point on E_8.

2. Prove that one must blow up twice to get an exceptional curve E_{10} along which $m_{10}(f_x) = m_{10}(f_y)$, which resolves the linear system and, that this gives the resolution graph Γ' of Figure 25.

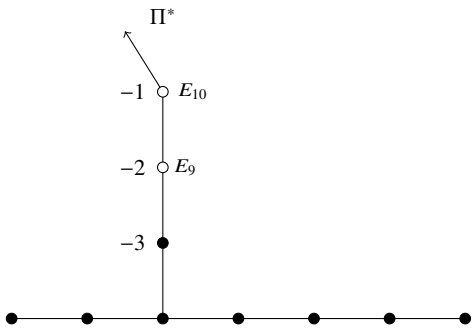


Fig. 25: The graph Γ'

Now, consider the computation of the resolution of E_8 by Laufer's method (see Appendix 5) which consists of computing the double over $\ell\colon (X,0) \to (\mathbb{C}^2,0)$ branched over the discriminant curve $\Delta\colon y^3 + z^5 = 0$. We start with the minimal resolution $\sigma'\colon Y' \to \mathbb{C}^2$ of Δ, and we see from the computation of self-intersections given in 5 that we need to blow up five times the strict transform Δ^* in order to get the resolution graph Γ'. The resulting map is the morphism $\sigma\colon Y \to \mathbb{C}^2$ which resolves the base points of the family of projected polar curves $(\ell(\Pi_{\mathcal{D}}))_{\mathcal{D}\subset\Omega}$. The morphism σ is a composition of blow-ups of points and the last exceptional curve created in the process is the Δ-curve. Its inner rate is $\frac{5}{3} + 5.\frac{1}{3} = \frac{10}{3}$.

The geometric decomposition of $\mathbb{C}^2$ associated with ℓ is described by the resolution tree of σ with nodes weighted by the inner rates (Figure 26).

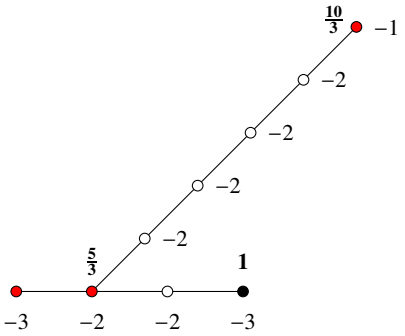


Fig. 26: Geometric decomposition of $(\mathbb{C}^2,0)$ associated with ℓ

Notice that the inner rate of the Δ-curve, which is also the inner rate of the curve $E_{\nu_{10}}$ of $\pi^{-1}(0)$ can also be computing using the equations as follows. For a generic $(a,b) \in \mathbb{C}^2$, $x + ay^2 + bz^4 = 0$ is the equation of the polar curve $\Pi_{a,b}$ of a generic projection. The image $\ell(\Pi_{a,b}) \subset \mathbb{C}^2$ under the projection $\ell = (y,z)$ has equation

$$y^3 + a^2y^4 + 2aby^2z^4 + z^5 + b^2z^8 = 0$$

The discriminant curve $\Delta = \ell(\Pi_{0,0})$ has Puiseux expansion $y = (-z)^{\frac{5}{3}}$, while for $(a,b) \neq (0,0)$, we get for $\ell(\Pi_{a,b})$ a Puiseux expansion $y = (-z)^{\frac{5}{3}} - \frac{a^2}{3}z^{\frac{10}{3}} + \cdots$. So the discriminant curve Δ has highest characteristic exponent $\frac{5}{3}$ and its contact exponent with a generic $\ell(\Pi_{a,b})$ is $\frac{10}{3}$.

By construction, the projection $\ell(W)$ of a polar wedge W is a union of D-pieces which refines the geometric decomposition of $(\mathbb{C}^2,0)$ associated with ℓ. By Lemma 3.29, which guarantees that ℓ is a local bilipschitz homeomorphism for the inner metric outside W, any piece of this geometric decomposition outside the polar wedge W lifts to a piece of the same type. We obtain a geometric decomposition of $\overline{X \setminus W}$. Finally, the Polar Wedge Lemma 4.15 says that W is a union of D-pieces whose fibrations match with those of its neighbour B-pieces in $\overline{X \setminus W}$. We obtain the following result:

Proposition 4.20. *Each $B(q)$-piece (resp. $A(q,q')$-piece) of the geometric decomposition of $(\mathbb{C}^2,0)$ associated with ℓ lifts by ℓ to a union of $B(q)$-pieces (resp. $A(q,q')$-pieces) in $(X,0)$ (with the same rates).*

Therefore, we obtain a geometric decomposition of $(X,0)$ into a union of B-pieces and A-pieces obtained by lifting by ℓ the A- and B-pieces of the geometric decomposition of $(\mathbb{C}^2,0)$ associated with ℓ.

Definition 4.21. We call this decomposition the *initial geometric decomposition* of $(X,0)$.

Example 4.22. The initial geometric decomposition of the surface germ E_8 is represented by the graph of Figure 27. The vertices corresponding to the $B(\frac{5}{3})$-piece and the $B(\frac{10}{3})$-piece are in red, the $\mathcal{L}$-node is in black, the white vertices correspond to the A-pieces.

We will now amalgamate some pieces to define the *inner geometric decomposition* of $(X,0)$. We first need to specify some special vertices in the resolution graph.

Definition 4.23 (Nodes). Let $\pi\colon Z \to X$ be a resolution of $(X,0)$ which factors through the blow-up of the maximal ideal $e_0\colon X_0 \to X$ and through the Nash modification. Let Γ be the dual resolution graph of π.

We call *$\mathcal{L}$-curve* any component of $\pi^{-1}(0)$ which corresponds to a component of $e_0^{-1}(0)$ and *$\mathcal{L}$-node* any vertex of Γ which represents an $\mathcal{L}$-curve.

We call *special $\mathcal{P}$-curve* any component E_i of $\pi^{-1}(0)$ which corresponds to a component of $\nu^{-1}(0)$ (i.e., it intersects the strict transform of the polar curve Π) and such that

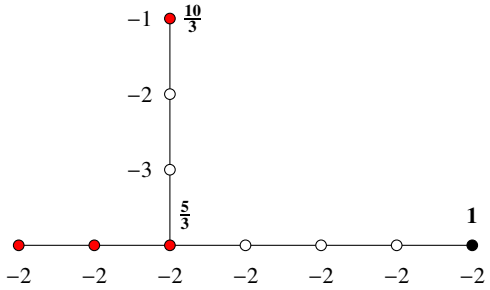


Fig. 27: Initial geometric decompostion for the singularity E_8

1. The curve E_i intersects exactly two other components of E_j and E_k of $\pi^{-1}(0)$;
2. The inner rates satisfy: $max(q_{E_j}, q_{E_k}) < q_{E_i}$.

We call *special $\mathcal{P}$-node* any vertex of Γ which represents a special $\mathcal{P}$-curve.

We call *inner node* any vertex of Γ which has at least three incident edges or which represents a curve with genus > 0 or which is an $\mathcal{L}$- or a special $\mathcal{P}$-node.

Using Lemma 4.11, we now amalgamate iteratively D and A-pieces but with the rule that we never amalgamate the special A-pieces with a neighbouring piece.

Definition 4.24. We call this decomposition the *inner geometric decomposition* of $(X, 0)$.

The following is a straightforward consequence of this amalgamation rule. The pieces of the inner geometric decomposition of $(X, 0)$ can be described as follows:

Proposition 4.25. *For each inner node (i) of Γ, let Γ_i be the subgraph of Γ consisting of (i) union any attached bamboo.*

1. *The B-pieces are the sets $B_i = \pi(\mathcal{N}(\Gamma_i))$, in bijection with the inner nodes of Γ. Moreover, for each node (i), B_i is a $B(q_i)$-piece, where q_i is the inner rate of the exceptional curve represented by (i) and the link $B_i^{(\epsilon)}$ is a Seifert manifold.*
2. *The A-pieces are the sets $A_{i,j} = \pi(N(S_{i,j}))$ where $S_{i,j}$ is a string or an edge joining two nodes (i) and (j) of Γ. Moreover, $A_{i,j}$ is an $A(q_i, q_j)$-piece and the link $A_{i,j}^{(\epsilon)}$ is a thickened torus having a common boundary component with both $B_i^{(\epsilon)}$ and $B_j^{(\epsilon)}$.*

In particular, the inner geometric decomposition of $(X, 0)$ induces a graph decomposition of the link $X^{(\epsilon)}$ whose Seifert components are the links $B_i^{(\epsilon)}$ and the separating tori are in bijection with the thickened tori $A_{i,j}^{(\epsilon)}$.

Remark 4.26. The inner geometric decomposition is a refinement of the thick-thin decomposition. Indeed, the thick part is the union of the $B(1)$-pieces and adjacent $A(1, q)$-pieces, and the thin part is the union of the remaining pieces.

Example 4.27. The inner geometric decomposition of the surface germ E_8 is represented by the graph of Figure 28. The vertices corresponding to the $B(\frac{5}{3})$-piece are in red, the $\mathcal{L}$-node is in black, the white vertices correspond to the A-piece.

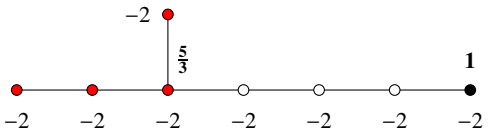


Fig. 28: Inner geometric decompostion for the singularity E_8

Exercise 4.28. Draw the resolution graph with inner rates at inner nodes representing the inner geometric decomposition of the surface germ $z^2 + f(x, y) = 0$ where $f(x, y) = 0$ is the plane curve with Puiseux expansion $y = x^{\frac{3}{2}} + x^{\frac{7}{4}}$.

Example 4.29. Here is an example with a special $\mathcal{P}$-node. This is a minimal surface singularity (see [Kol85]). Minimal singularities are special rational singularities which play a key role in resolution theory of surfaces, and they also share a remarkable metric property, as shown in [NPP19b]: they are Lipschitz normally embedded, i.e., their inner and outer metrics are Lipschitz equivalent. We refer to [NPP19b] for details on minimal singularities and for the computations on this particular example.

Consider the minimal surface singularity given by the minimal resolution graph of Figure 29. The $\mathcal{L}$-nodes are the black vertices.

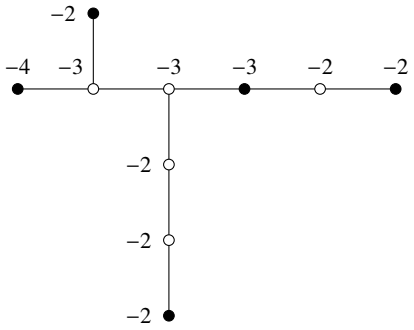


Fig. 29: Minimal resolution of a minimal surface singularity

As shown in [NPP19b], one has to blow up once to obtain the minimal resolution which factors through Nash modification, creating the circled vertex on the graph of Figure 30. The arrows on this graph correspond to the components of the polar curve. The inner rates (in bold) are computed in [NPP19b]. We obtain two special $\mathcal{P}$-nodes (the blue vertices).

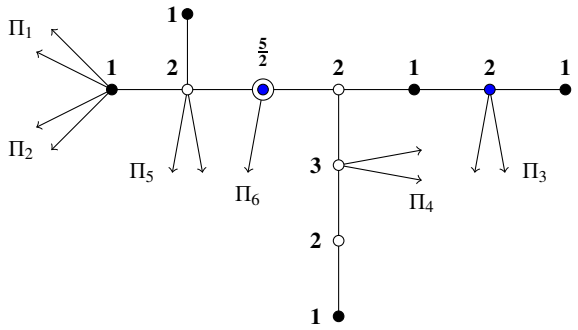


Fig. 30: $\mathcal{P}$-nodes and resolution of the generic polar curve

We then obtain the inner geometric decomposition described on Figure 31. There are nine inner nodes, which correspond to five $B(1)$-pieces (in black), two special A-pieces with rates $\frac{5}{2}$ and 2 (in blue) and two $B(2)$-pieces (in red).

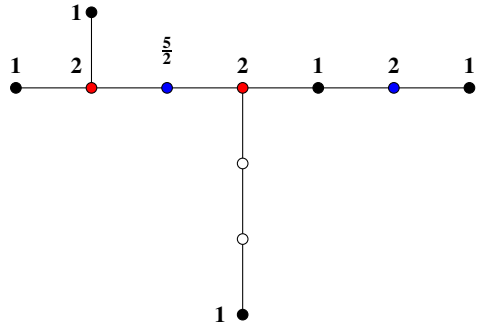


Fig. 31: Minimal resolution which factors through Nash transform

The terminology *inner geometric decomposition* comes from the following result:

Theorem 4.30 ([BNP14] Complete Classification Theorem for inner Lipschitz geometry). *The inner Lipschitz geometry of* $(X, 0)$ *determines and is uniquely determined by the following data:*

1. *The graph decomposition of* $X^{(\epsilon)}$ *as the union of the links* $B_i^{(\epsilon)}$ *and* $A_{i,j}^{(\epsilon)}$.
2. *for each* $B_i^{(\epsilon)}$, *the inner rate* $q_i \geq 1$.
3. *for each* $B_i^{(\epsilon)}$ *such that* $q_i > 1$, *the homotopy class of the foliation by fibers of the fibration* $z_1 \colon B_i^{(\epsilon)} \to S^1_\epsilon$.

Moreover, these data are completely encoded in the resolution graph Γ *whose nodes are weighted by the rates* q_i *and by the multiplicities of a generic linear form* h *along*

the exceptional curves E_i up to a multiplicative constant. The latter is equivalent to the data of the maximal ideal Z_{max} (see [Nem99]) up to a multiple.

4.5 The outer Lipschitz decomposition

We now define on $(X, 0)$ a geometric decomposition of $(X, 0)$ which is a refinement of the inner geometric decomposition.

Definition 4.31. We use again the notations of Definition 4.23. We call $\mathcal{P}$*-curve* any component of $\pi^{-1}(0)$ which corresponds to a component of $\nu^{-1}(0)$ and $\mathcal{P}$*-node* any vertex of Γ which represents a $\mathcal{P}$-curve. We call *outer node* any vertex of Γ which has at least three incident edges or which represents a curve with genus > 0 or which is an $\mathcal{L}$- or a $\mathcal{P}$-node.

We start again with the initial geometric decomposition of $(X, 0)$ (Definition 4.21). Using Lemma 4.11, we amalgamate iteratively D and A-pieces but with the rule that we never amalgamate any B-pieces corresponding to a $\mathcal{P}$-node.

Definition 4.32. We call this decomposition the *outer geometric decomposition* of $(X, 0)$.

Let us now state an analog of Proposition 4.25:

Proposition 4.33. *The pieces of the outer geometric decomposition of $(X, 0)$ can be described as follows. For each outer node (i) of Γ, let Γ_i be the subgraph of Γ consisting of (i) and any attached bamboo.*

1. *The B-pieces are the sets $B_i = \pi(\mathcal{N}(\Gamma_i))$, in bijection with the outer nodes of Γ, and B_i is a $B(q_i)$-piece.*
2. *The A-pieces are the sets $A_{i,j} = \pi(N(S_{i,j}))$ where $S_{i,j}$ is a string or an edge joining two outer nodes i and j of Γ. Moreover, $A_{i,j}$ is an $A(q_i, q_j)$-piece.*

Example 4.34. The outer decomposition of the minimal singularity of Example 4.29 is described on Figure 32. There is exactly one outer node which is not an inner node. So the outer decomposition is a refinement of the inner one: there is an extra $B(3)$-piece.

Example 4.35. The outer geometric decomposition of the E_8 singularity coincides with the initial geometric decomposition. So its graph is the one of Example 4.22. Notice that the E_8 example is very special. In general the outer geometric decomposition has much less pieces than the initial geometric decomposition.

Theorem 4.36. *The outer Lipschitz geometry of a normal surface singularity $(X, 0)$ determines the geometric decomposition of $(X, 0)$ up to self-bilipschitz homeomorphism.*

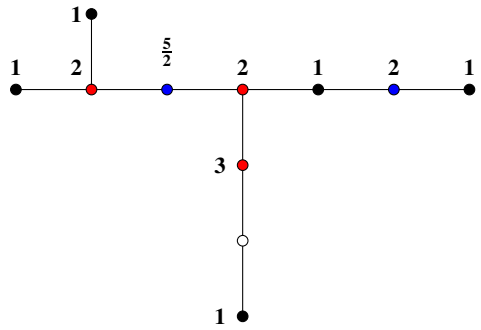


Fig. 32

Moreover, these data are completely encoded in the resolution graph Γ *where each outer node is weighted by the inner rate* q_{E_i} *and the self-intersection* E_i^2 *of the corresponding exceptional curve* E_i *and by the multiplicity* m_i *of a generic linear form* h *along* E_i.

Notice that the latter is equivalent to the datum of the maximal ideal cycle $Z_{max} := \sum_i m_i E_i$ *in the resolution* π. *(see [Nem99, 2.I] for details on* Z_{max}*).*

The statement of Theorem 4.36 has some similarities with that of Theorem 4.30, but the proof is radically different. The proof of the Lipschitz invariance of the outer geometric decomposition is based on a bubble trick which enables one to recover first the B-pieces of the decomposition which have highest inner rate. Then the whole decomposition is determined by an inductive process based again on a second bubble trick by exploring the surface with bubbles having radius ϵ^q, with decreasing rates q. The proof is delicate. We refer to [NP12] for details.

Remark 4.37. As a byproduct of the bilipschitz invariance of the maximal ideal cycle Z_{max} stated in Theorem 4.36 we obtain that the multiplicity $m(X, 0)$ is an invariant of the Lipschitz geometry of a complex normal surface germ. Indeed, $m(X, 0)$ is nothing but the sum of the multiplicities of Z_{max} at the $\mathcal{L}$-nodes of Γ.

In [FdBFS18], the authors prove a broad generalization of this fact: the outer Lipschitz geometry of a surface singularity (not necessarily normal) determines its multiplicity

The Lipschitz invariance of the multiplicity is no longer true in higher dimension as proved in [BFSV18]. Actually, the proofs of the bilipschitz invariance in [NP12] and [FdBFS18] deeply use the classification of 3-dimensional manifolds up to diffeomorphisms.

Using again bubble tricks, we can prove that beyond the weighted graph Γ and the maximal cycle Z_{max}, the outer Lipschitz geometry determines a large amount of other classical analytic invariants. These invariants are of two types. The first is related to the generic hyperplane sections and the blow-up of the maximal ideal, and the second is related to the polar and discriminant curves of generic plane projections and the Nash modification:

Theorem 4.38. *[NP12] If $(X,0)$ is a normal complex surface singularity, then the outer Lipschitz geometry on X determines:*

1. **Invariants from generic hyperplane sections:**
   a. *the decoration of the resolution graph Γ by arrows corresponding to the strict transform of a generic hyperplane section (these data are equivalent to the maximal ideal cycle Z_{max});*
   b. *for a generic hyperplane H, the outer Lipschitz geometry of the curve $(X \cap H, 0)$.*
2. **Invariants from generic plane projections:**
   a. *the decoration of the resolution graph Γ by arrows corresponding to the strict transform of the polar curve of a generic plane projection;*
   b. *the embedded topology of the discriminant curve of a generic plane projection;*
   c. *the outer Lipschitz geometry of the polar curve of a generic plane projection.*

5 Appendix: the resolution of the E8 surface singularity

In this appendix, we explain how to compute the minimal resolution graph of a singularity with equation of the form $z^2 + f(x,y) = 0$ by Laufer's method, described in [Lau71, Chapter 2] (page 23 to 27 for the E_8 singularity). Here we will just introduce the method and perform it in the particular case of E_8. We invite the reader to study it in [Lau71].

Laufer's method is based on the Hirzebruch-Jung algorithm which resolves any surface singularity.

5.1 Hirzebruch-Jung algorithm

We refer to the paper [PP11] of Patrick Popescu-Pampu for more details on this part. The Hirzebruch-Jung algorithm consists in considering a finite morphism $\ell\colon (X,0) \to (\mathbb{C}^2,0)$. Then one takes a resolution $\sigma\colon Y \to \mathbb{C}^2$ of the discriminant curve Δ of ℓ, one resolves the singularities of Δ and one considers the pull-back $\widetilde{\sigma}\colon Z \to X$ of σ by ℓ. We then also have a finite morphism $\widetilde{\ell}\colon Z \to Y$ such that $\sigma \circ \widetilde{\ell} = \widetilde{\sigma} \circ \ell$. Let $n\colon Z_0 \to Z$ be the normalization of Z.

The singularities of Z_0 are quasi-ordinary singularities relative to the projection $\widetilde{\ell} \circ n\colon Z_0 \to Y$ and with discriminant the singularities of the curve $\sigma^{-1}(\Delta)$, which are ordinary double points. Resolving these remaining singularities, one gets a morphism $\alpha\colon Z \to Z_0$. The composition $\pi = \widetilde{\sigma} \circ \alpha\colon Z \to X$ is a resolution of $(X,0)$ (in general far from being minimal).

5.2 Laufer's method

It resolves the surface germ $(X,0)\colon x^2+f(y,z)=0$ by applying Hirzebruch-Jung algorithm with the projection $\ell\colon (x,y,z)\mapsto(y,z)$ and then by giving an easy way to compute Z from a specific resolution tree T of the discriminant curve $\Delta\colon f(y,z)=0$ of ℓ.

Let us explain it on the singularity E_8. The discriminant Δ of the projection $\ell\colon (X,0)\to(\mathbb{C}^2,0)$ has equation $f(y,z)=0$ where $f(y,z)=y^3+z^5$. We start with the minimal resolution $\sigma\colon Y\to\mathbb{C}^2$ of Δ. Its exceptional divisor consists in four curves $E_1,\dots,E_4$ labelled in their order of occurence in the sequence of blow-ups. Let m_i be the multiplicity of the function f along E_i. The integer m_i is defined as the exponent u^{m_i} appearing in the total transform of f by σ in coordinates centered at a smooth point of E_i, where $u=0$ is the local equation of E_i. So it can be computed when performing the sequence of blow-ups resolving $f=0$.

By [Lau71, Theorem 2.6] these multiplicities can also be computed from the self-intersections E_j^2 using the fact that for each $j=1,\dots,4$, the intersection $(\sigma^*f).E_j$ in Y equals 0, where $(\sigma^*f)=m_1E_1+\ldots+m_4E_4+f^*$, with f^* the strict transform of $f=0$ by σ.

One obtains the following resolution tree T on which each vertex (i) is weighted by the self intersection E_i^2 and by the multiplicity m_i (into parenthesis). The arrow represents the strict transform of Δ.

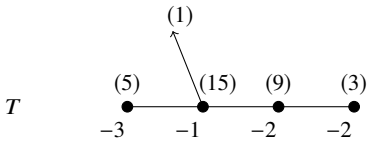


Fig. 33: The minimal resolution tree of $y^3+z^5=0$

Now, we blow up any intersection point between two components of the total transform (σ^*f) having both even multiplicities. In the case of E_8, all the multiplicities are even, so we blow up every double point of (σ^*f). We obtain the resolution tree T' of Figure 34.

In the particular case where there are no adjacent vertices having both odd multiplicities (this is the case in the above tree T'), a resolution graph Γ of $(X,0)\colon x^2=f(y,z)$ is obtained as follows: Γ is isomorphic to T', and for any vertex (i) of T', the corresponding vertex of Γ carries self-intersection $2E_i^2$ if the multiplicity m_i is odd and $\frac{1}{2}E_i^2$ if it is even. Moreover, the multiplicity of the function $f\circ\ell\colon (X,0)\to(\mathbb{C},0)$ is m_i if m_i is odd and $\frac{1}{2}m_i$ if m_i is even. In the case of E_8, we obtain the resolution graph Γ of Figure 35, where the arrow represents the strict transform of $f\circ\ell\colon (X,0)\to(\mathbb{C},0)$.

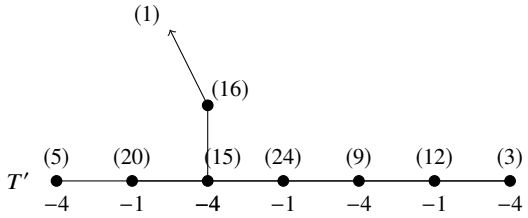


Fig. 34

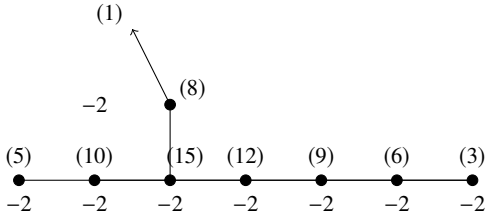


Fig. 35: The resolution graph Γ for E_8 with multiplicities of $y^3 + z^5$

There are no -1-exceptional curves which could be blown down. So forgetting f and its multiplicities we get the well known graph of the minimal resolution of E_8 (Figure 36).

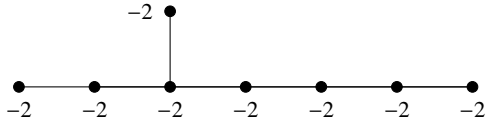


Fig. 36: The resolution minimal graph for E_8

In the case where some consecutive vertices have multiplicities which are odd, some vertices of T' may give two vertices in Γ. We refer to [Lau71] for details.

References

BF08. Lev Birbrair and Alexandre Fernandes. Inner metric geometry of complex algebraic surfaces with isolated singularities. *Comm. Pure Appl. Math.*, 61(11):1483–1494, 2008. 17

BFN08. Lev Birbrair, Alexandre Fernandes, and Walter D. Neumann. Bi-Lipschitz geometry of weighted homogeneous surface singularities. *Math. Ann.*, 342(1):139–144, 2008. 17

BFN09. Lev Birbrair, Alexandre Fernandes, and Walter D. Neumann. Bi-Lipschitz geometry of complex surface singularities. *Geom. Dedicata*, 139:259–267, 2009. 17

BFN10. Lev Birbrair, Alexandre Fernandes, and Walter D. Neumann. Separating sets, metric tangent cone and applications for complex algebraic germs. *Selecta Math. (N.S.)*, 16(3):377–391, 2010. 17

BFSV18. Lev Birbrair, Alexandre Fernandes, Jose Edson Sampaio, and Misha Verbitsky. Multiplicity of singularities is not a bi-lipschitz invariant. *arXiv preprint arXiv:1801.06849*, 2018. 6, 45

BNP14. Lev Birbrair, Walter D. Neumann, and Anne Pichon. The thick-thin decomposition and the bilipschitz classification of normal surface singularities. *Acta Math.*, 212(2):199–256, 2014. 2, 17, 18, 19, 21, 22, 23, 24, 30, 31, 32, 34, 37, 43

BS75. Joël Briançon and Jean-Paul Speder. La trivialité topologique n'implique pas les conditions de Whitney. *C. R. Acad. Sci. Paris Sér. A-B*, 280(6):Aiii, A365–A367, 1975. 24

Dur79. Alan H. Durfee. Fifteen characterizations of rational double points and simple critical points. *Enseign. Math. (2)*, 25(1-2):131–163, 1979. 23

Dur83. Alan H. Durfee. Neighborhoods of algebraic sets. *Trans. Amer. Math. Soc.*, 276(2):517–530, 1983. 19

EN85. David Eisenbud and Walter Neumann. *Three-dimensional link theory and invariants of plane curve singularities*, volume 110 of *Annals of Mathematics Studies*. Princeton University Press, Princeton, NJ, 1985. 28, 35

FdBFS18. Javier Fernández de Bobadilla, Alexandre Fernandes, and J. Edson Sampaio. Multiplicity and degree as bi-Lipschitz invariants for complex sets. *J. Topol.*, 11(4):958–966, 2018. 6, 45

FdBHPPS19. Javier Fernández de Bobadilla, Sonja Heinze and Maria Pe Pereira and Jose Edson Sampaio. Moderately Discontinuous Homology. preprint arXiv1910.12552. 28 October 2019. 1

Fer03. Alexandre Fernandes. Topological equivalence of complex curves and bi-Lipschitz homeomorphisms. *Michigan Math. J.*, 51(3):593–606, 2003. 9, 10

GBGPPP19. Evelia R. García Barroso, Pedro D. González Pérez, and Patrick Popescu-Pampu. The valuative tree is the projective limit of Eggers-Wall trees. *Rev. R. Acad. Cienc. Exactas Fís. Nat. Ser. A Mat. RACSAM*, 113(4):4051–4105, 2019. 8

GBT99. Evelia García Barroso and Bernard Teissier. Concentration multi-échelles de courbure dans des fibres de Milnor. *Comment. Math. Helv.*, 74(3):398–418, 1999. 28

HP03. J-P. Henry and A. Parusiński. Existence of moduli for bi-Lipschitz equivalence of analytic functions. *Compositio Math.*, 136(2):217–235, 2003. 1

KL77. Tzee Char Kuo and Yung Chen Lu. On analytic function germs of two complex variables. *Topology*, 16(4):299–310, 1977. 8

KO97. Krzysztof Kurdyka and Patrice Orro. Distance géodésique sur un sous-analytique. volume 10, pages 173–182. 1997. Real algebraic and analytic geometry (Segovia, 1995). 27

Kol85. János Kollár. Toward moduli of singular varieties. *Compositio Math.*, 56(3):369–398, 1985. 42

Lau71. Henry B. Laufer. *Normal two-dimensional singularities*. Princeton University Press, Princeton, N.J.; University of Tokyo Press, Tokyo, 1971. Annals of Mathematics Studies, No. 71. 38, 46, 47, 48

Mos85. Tadeusz Mostowski. Lipschitz equisingularity. *Dissertationes Math. (Rozprawy Mat.)*, 243:46, 1985. 6

Nem99. A. Némethi. Five lectures on normal surface singularities. In *Low dimensional topology (Eger, 1996/Budapest, 1998)*, volume 8 of *Bolyai Soc. Math. Stud.*, pages 269–351. János Bolyai Math. Soc., Budapest, 1999. With the assistance of Ágnes Szilárd and Sándor Kovács. 44, 45

NP12. Walter D. Neumann and Anne Pichon. Lipschitz geometry of complex surfaces: analytic invariants and equisingularity. *arXiv preprint arXiv:1211.4897*, 2012. 1, 2, 6, 10, 45, 46

NP14. Walter D. Neumann and Anne Pichon. Lipschitz geometry of complex curves. *J. Singul.*, 10:225–234, 2014. 1, 9, 13

NPP19a. Walter D. Neumann, Helge Møller Pedersen, and Anne Pichon. A characterization of lipschitz normally embedded surface singularities. *arXiv preprint arXiv:1806.11240*, 2019. To appear in *J. London Math. Soc.* . 28, 37

NPP19b. Walter D. Neumann, Helge Møller Pedersen, and Anne Pichon. Minimal surface singularities are lipschitz normally embedded. *arXiv preprint arXiv:1503.03301*, 2019. To appear in *J. London Math. Soc.* . 42

Par88. Adam Parusiński. Lipschitz properties of semi-analytic sets. *Ann. Inst. Fourier (Grenoble)*, 38(4):189–213, 1988. 6

Par94. Adam Parusiński. Lipschitz stratification of subanalytic sets. *Ann. Sci. École Norm. Sup. (4)*, 27(6):661–696, 1994. 6

PP11. Patrick Popescu-Pampu. Introduction to Jung's method of resolution of singularities. In *Topology of algebraic varieties and singularities*, volume 538 of *Contemp. Math.*, pages 401–432. Amer. Math. Soc., Providence, RI, 2011. 29, 46

PT69. Frédéric Pham and Bernard Teissier. Fractions lipschitziennes d'une algèbre analytique complexe et saturation de zariski. *Prépublications Ecole Polytechnique*, (M17.0669), 1969. 9

Sam17. Jose Edson Sampaio. Multiplicity, regularity and blow-spherical equivalence of complex analytic sets. *arXiv preprint arXiv:1702.06213*, 2017. 6

Spi90. Mark Spivakovsky. Sandwiched singularities and desingularization of surfaces by normalized Nash transformations. *Ann. of Math. (2)*, 131(3):411–491, 1990. 22, 26

Tei82. Bernard Teissier. Variétés polaires. II. Multiplicités polaires, sections planes, et conditions de Whitney. In *Algebraic geometry (La Rábida, 1981)*, volume 961 of *Lecture Notes in Math.*, pages 314–491. Springer, Berlin, 1982. 8, 25

TMW89. Le Dung Trang, Françoise Michel, and Claude Weber. Sur le comportement des polaires associées aux germes de courbes planes. *Compositio Math.*, 72(1):87–113, 1989. 10

Wal04. C. T. C. Wall. *Singular points of plane curves*, volume 63 of *London Mathematical Society Student Texts*. Cambridge University Press, Cambridge, 2004. 8, 28, 35